Dynamos on galactic scales, or

Dynamos around us.

Part II. Observations of astrophysical velocity and magnetic fields

Anvar Shukurov

School of Mathematics and Statistics, Newcastle University, U.K.





1. Observations of astrophysical velocity and magnetic field

- 1.1. The Doppler shift of spectral lines and velocity measurements
- 1.2. Detection and measurement of astrophysical magnetic fields
 - (a) Zeeman splitting of spectral lines
 - (b) Faraday rotation of polarised emission
 - (c) Synchrotron emission
 - (d) Light polarization by interstellar dust

2. Galactic and extragalactic magnetic fields from observations

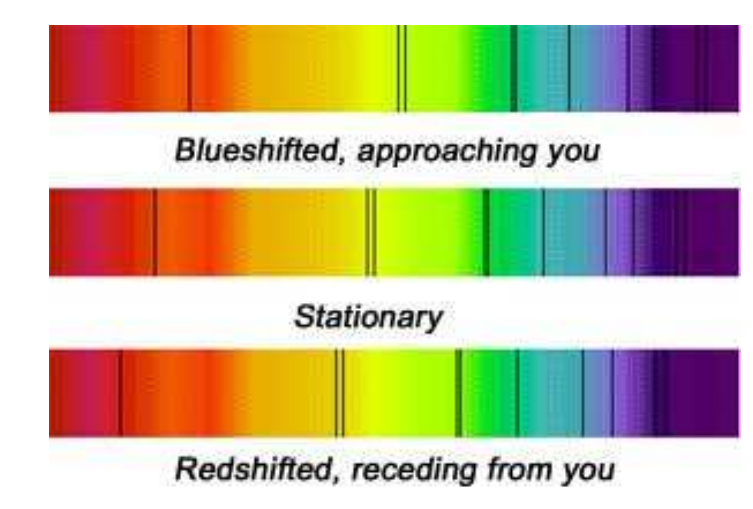
- 2.1. Spiral galaxies
- 2.2. Galaxy clusters
- 2.3. Briefly on accretion discs

1.1. The Doppler shift of spectral lines and velocity measurements

Change of a spectral line wavelength $\Delta\lambda$ when the radiation source moves towards or away from the observer at a speed v_s ($\ll c$):

$$z = \frac{\Delta \lambda}{\lambda_0} = \frac{v_s}{c},$$

 $z = \text{redshift}, \ \lambda_0 = \text{rest-frame wavelength}$



(wavelength increases, $\Delta\lambda > 0$ when the sources recedes, $v_s > 0$).

Doppler effect applet: http://www.astro.ubc.ca/~scharein/a311/Sim/doppler/Doppler.html

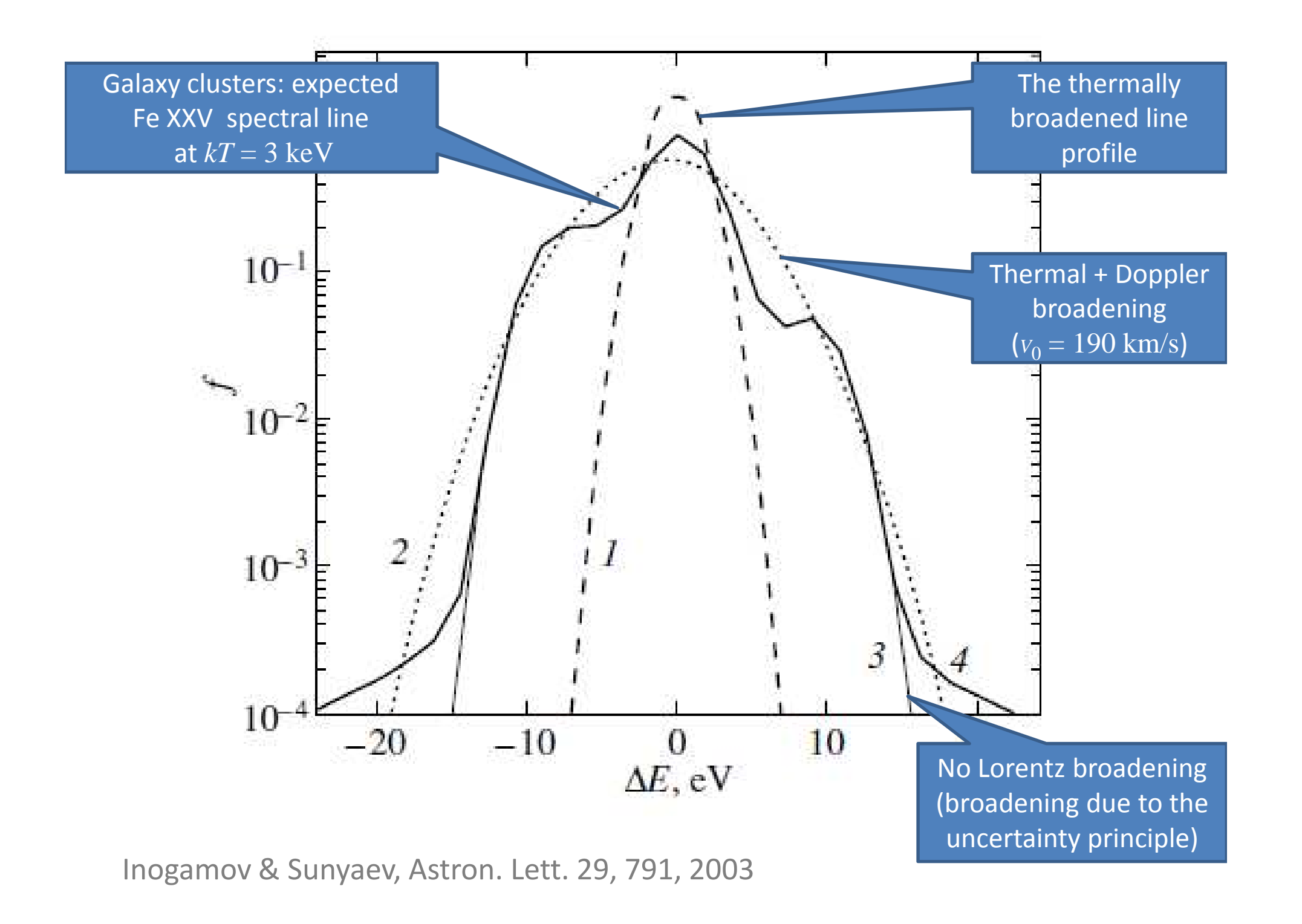
- □ Only the line-of-sight velocity is probed
 ⇒ model assumptions (e.g., pure rotation) used to deduce a 3D velocity field.
- □ Random motions (turbulence) ⇒ random Doppler shifts ⇒ broadening of spectral lines.

Line widths (in terms of frequency $\nu = 2\pi c/\lambda$):

thermal broadening:
$$\frac{\delta \nu}{\nu_0} = \frac{\sqrt{2kT/m_i}}{c}$$
,

hydrodynamic broadening:
$$\frac{\delta \nu}{\nu_0} = \frac{v_0}{c}$$
,

T= temperature, $m_i=$ emitting atom mass, $v_0=$ r.m.s. turbulent velocity.



1.2. Detection and measurement of astrophysical magnetic fields



- (a) Zeeman splitting of spectral lines
- (b) Faraday rotation of polarised emission
- (c) Synchrotron emission
- (d) Light polarization by interstellar dust
- (e) Other methods

(a) Zeeman splitting

Magnetic field splits atomic energy levels:

$$\Delta E = \pm \mu g M B$$

$$\mu = \frac{e\hbar}{2mc} = 9.3 \times 10^{-21} \, \mathrm{erg} \, \mathrm{G}^{-1} = \mathrm{Bohr's}$$
 magneton,

g = the Lande factor of the energy level (depends on the quantum numbers),

M= magnetic quantum number (projection of the total angular momentum on \vec{B}).

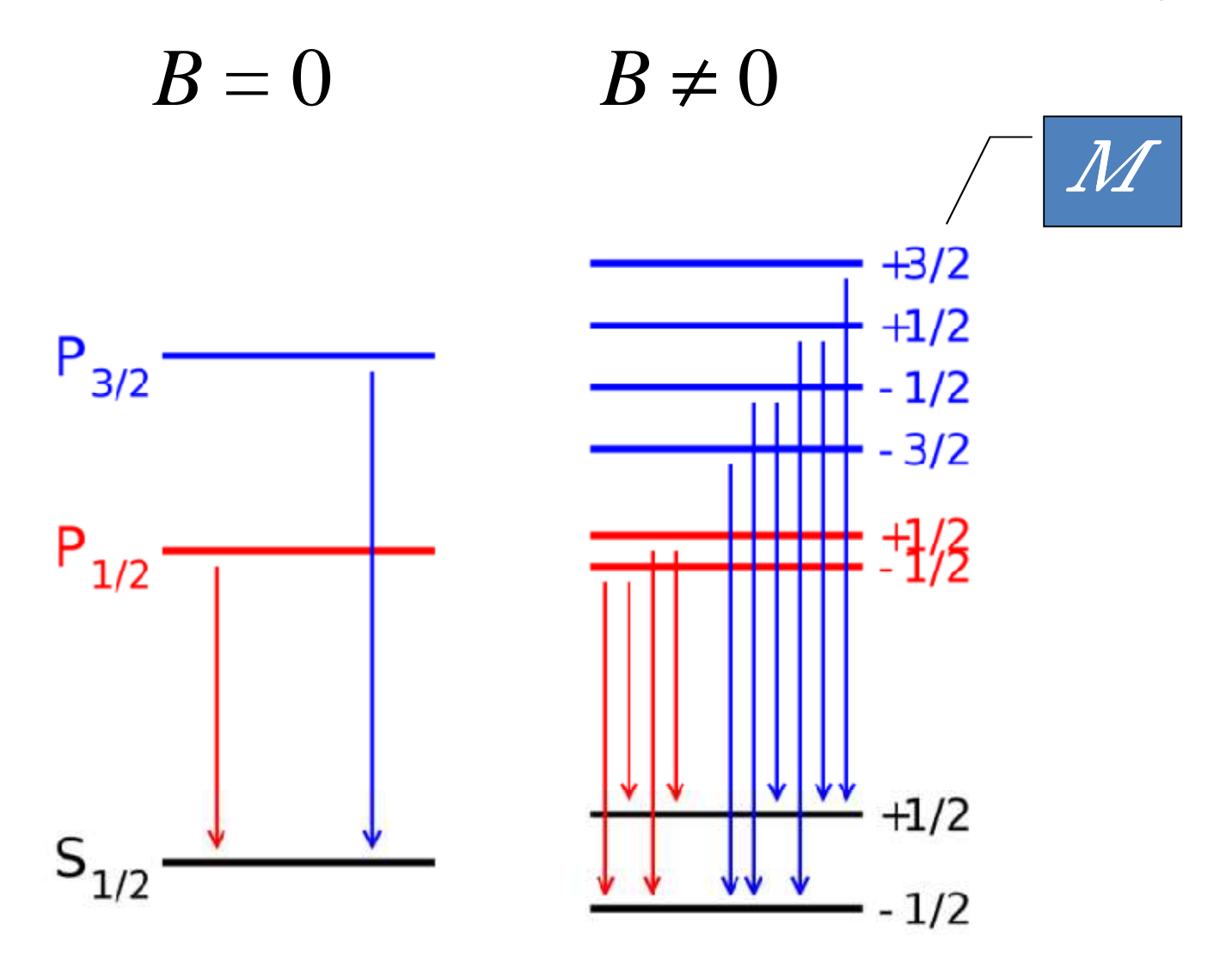
A spectral line is split into a multiplet,

$$\Delta \nu = 1.4 \times 10^6 \,\mathrm{Hz}\,\Delta(gM)\left(rac{B}{1\,\mathrm{G}}
ight),$$

with polarised components.

Thermal line broadening:
$$\Delta
u_T =
u_0 \frac{v_T}{c} \propto \sqrt{T}$$

Need $\Delta \nu >> \Delta \nu_T$ to detect the Zeeman splitting \Rightarrow observe cooler regions (absorption lines), carefully select the spectral lines to observe.

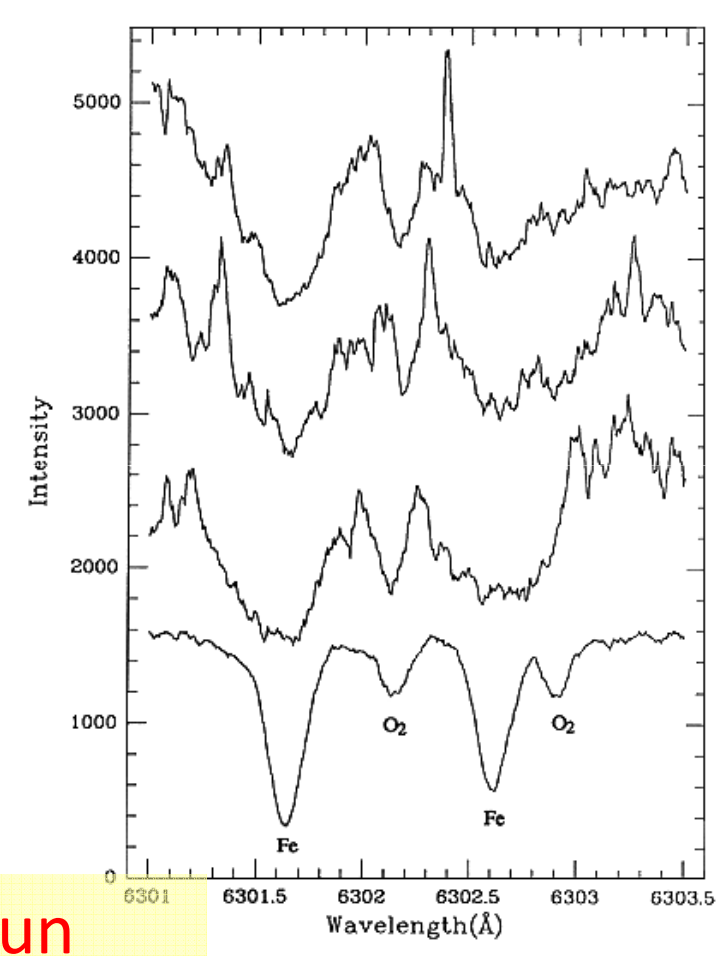


Hydrogen Ly α line: transitions $2P_{1/2} \rightarrow 1S_{1/2}$, $2P_{3/2} \rightarrow 1S_{1/2}$ (with spin-orbit interaction)

The Sun:

 $B > 1500 \text{ G} \Rightarrow \text{Zeeman splitting}$ (sunspots, $B \leq 3000 \text{ G}$, Hale 1908)

 $B < 1500 \text{ G} \Rightarrow \text{Zeeman broadening},$ polarimetry
(Babcock & Babcock 1952)



The most important method for the Sun

Solar spectrum near 6300 Å. **Top three**: a large sunspot, Zeeman-broadened Fe lines. **Bottom**: nearby bright photosphere, weak magnetic field.

Interstellar medium:

□Splitting of CO, CN molecular radio lines from dense star forming regions,

$$n = 10^5 - 10^6 \text{ cm}^{-3}, B > 1 \text{ mG}.$$

☐ Broadening of HI, OH lines, dense clouds,

$$n > 10 \text{ cm}^{-3}, B > 1 \mu\text{G}.$$

(b) Faraday rotation

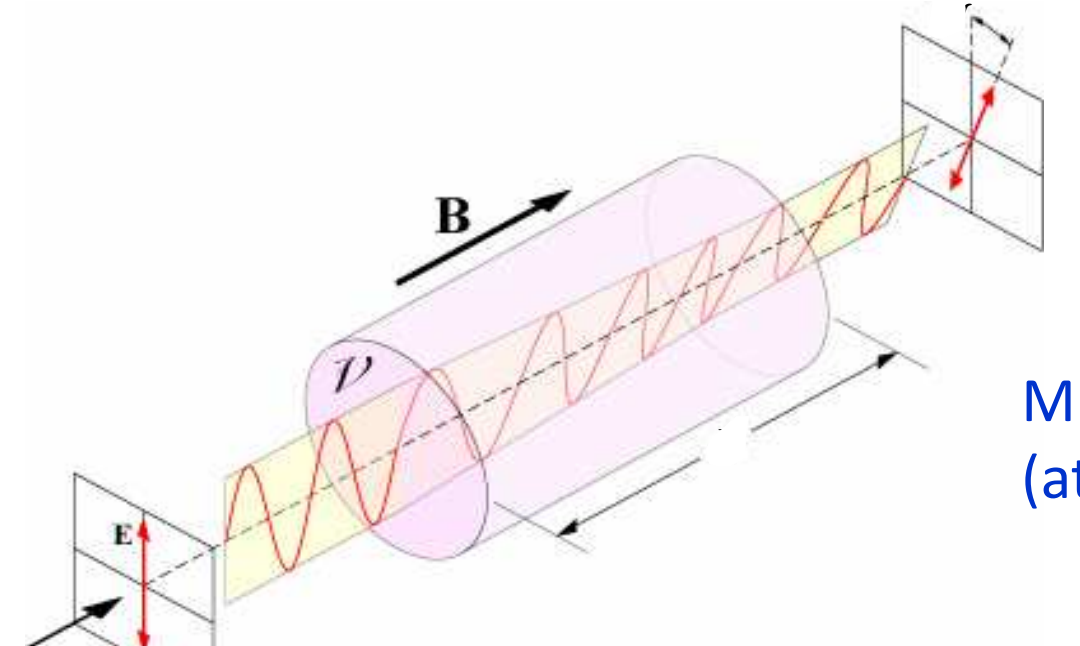
☐ Magnetic birefringence:

electromagnetic waves of left-handed and right-handed circular polarisations propagate through magnetised plasma at different phase speeds

(because electrons gyrate in a certain sense in given magnetic field)

☐ Linearly polarised wave = left + right circular polarizations

□⇒ Magnetic field turns the polarisation plane



Polarisation angle:

$$\psi = \psi_0 + RM \lambda^2$$

Multifrequency observations (at least two wavelengths):

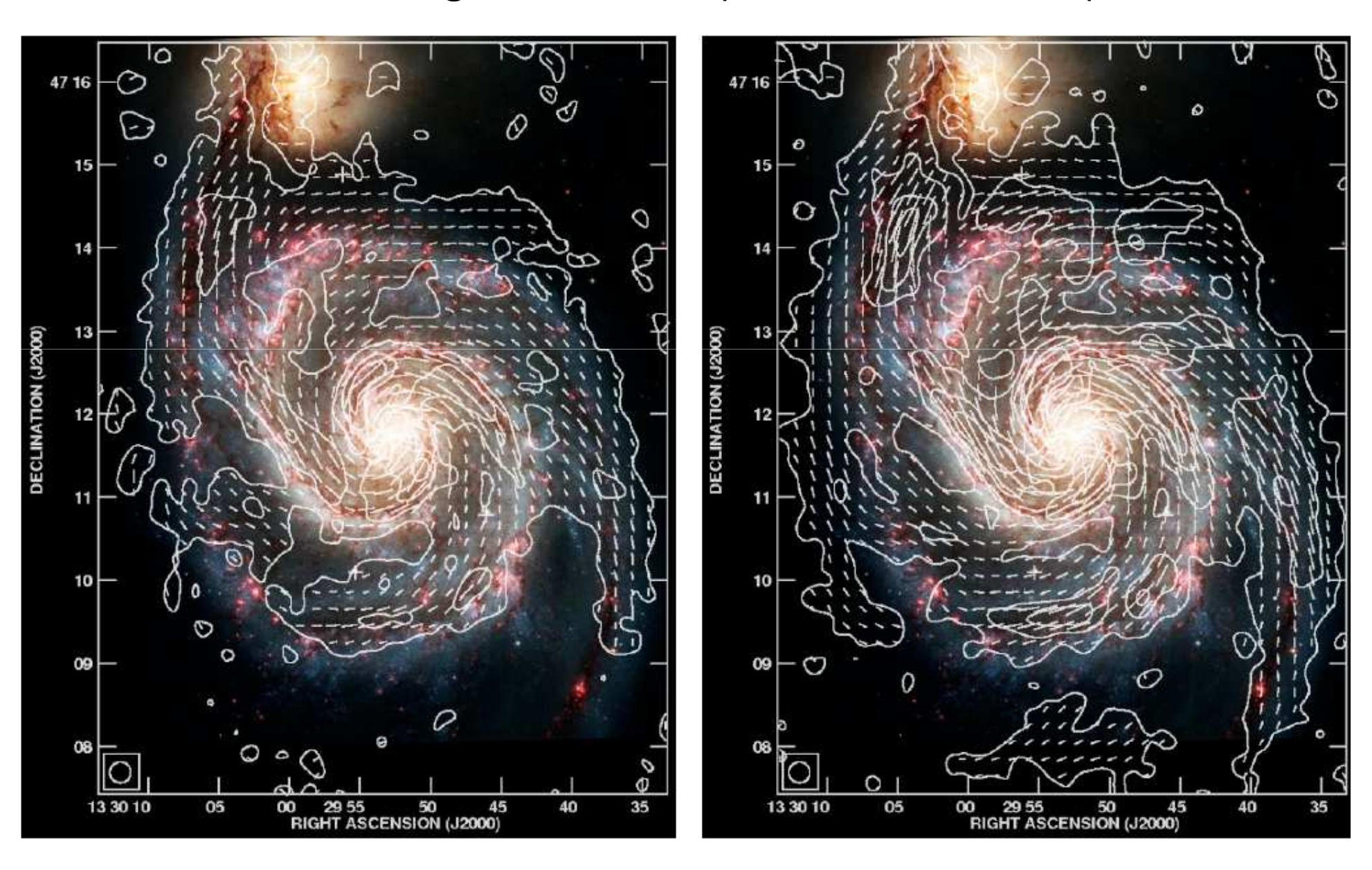
$$RM = \frac{\psi_1 - \psi_2}{\lambda_1^2 - \lambda_2^2}$$

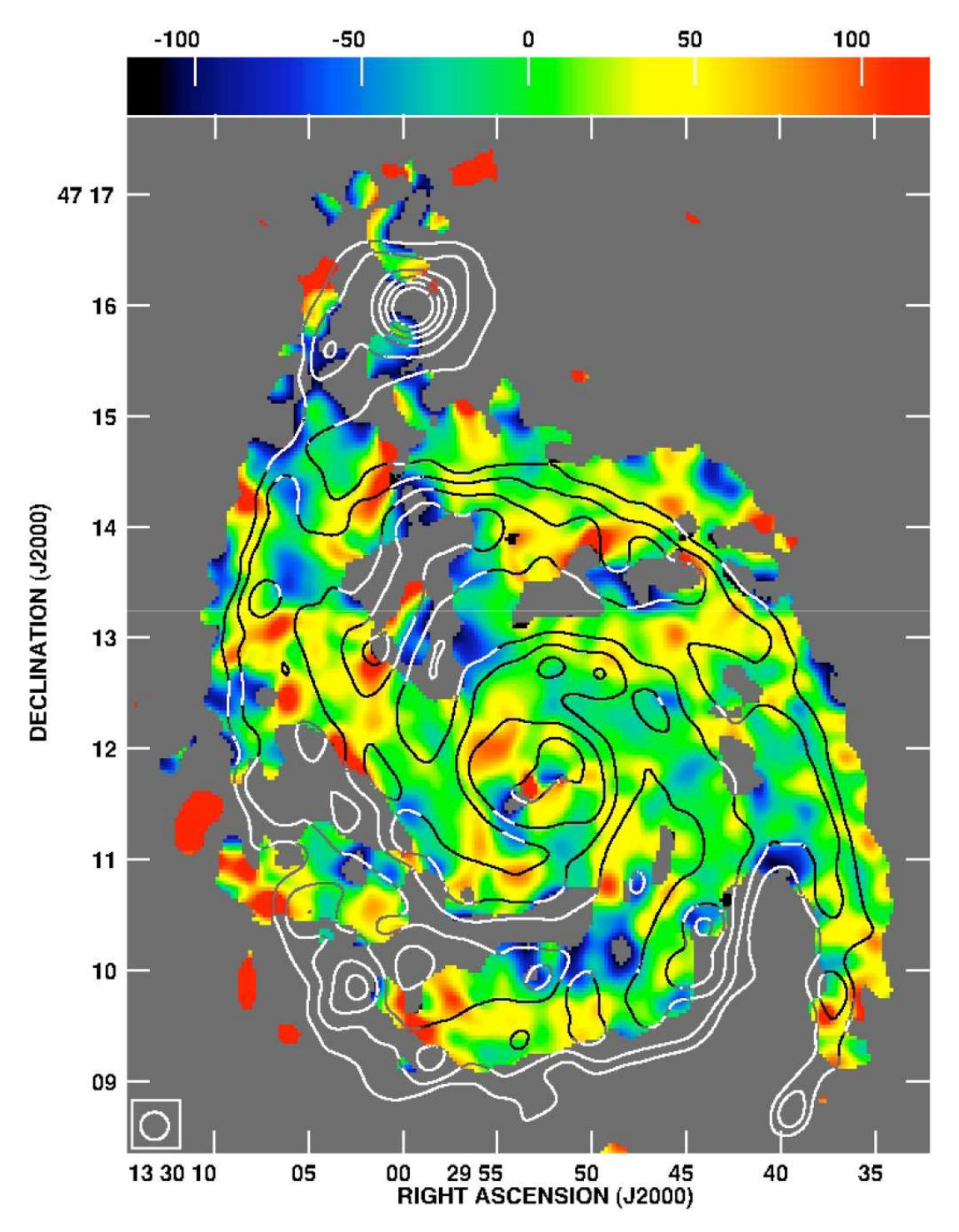
$$RM = \frac{e^3}{2\pi m_e^2 c^4} \int_0^L n_e \vec{B} \cdot \vec{s}$$

$$= 0.81 \frac{\text{rad}}{\text{m}^2} \int_0^L \frac{n_e}{1 \text{ cm}^{-3}} \frac{B_{\parallel}}{1 \mu \text{G}} \frac{ds}{1 \text{ pc}}.$$

RM is sensitive to the magnetic field direction, hence probes the large-scale magnetic field.

 $\lambda 3$ cm and (b) $\lambda 6$ cm (right) polarized radio emission at 15" resolution from VLA and Effelsberg observations (Fletcher et al., 2010)





Fletcher et al., 2010:

Rotation measure RM [rad/m²] between $\lambda 3$ cm and $\lambda 6$ cm, 15" resolution

+ contours of mid-infrared 15 μm emission (Sauvage et al. 1996)

Faraday rotation in a random magnetic field: the autocorrelation function of RM

- $\vec{r}=(x,y,z)$: Oz directed towards the observer, $\vec{X}=(X,Y)$: 2D frame in the sky plane.
- RM = $K \int_0^L n_e B_z dz$, $\langle B_z \rangle = 0$.
- The two-point correlation tensor of a statistically homogeneous, isotropic, mirror-symmetric, random magnetic field:

$$\langle B_i(\vec{x})B_j(\vec{y})\rangle = M_{ij}(r), \quad \vec{r} = \vec{x} - \vec{y}.$$

$$M_{ij} = \left(\delta_{ij} - \frac{r_i r_j}{r^2}\right) M_{\rm N}(r) + \frac{r_i r_j}{r^2} M_{\rm L}(r).$$

•
$$\nabla \cdot \vec{B} = 0 \quad \Rightarrow \quad M_{\rm N} = \frac{1}{2r} \frac{\partial}{\partial r} (r^2 M_{\rm L}).$$

• $n_e = \text{const}$ (subsonic turbulence).

Correlation function of RM

$$\zeta = z_1 - z_2, \quad R = |\vec{X}_1 - \vec{X}_2|, \quad r^2 = R^2 + \zeta^2, \quad Z = \frac{1}{2}(z_1 + z_2).$$

$$C(R) = \langle \text{RM}(\vec{X}_1) \text{RM}(\vec{X}_2) \rangle$$

$$= K^2 n_e^2 L \int_{-L}^{L} M_{zz}(R, \zeta) d\zeta$$

$$= K^2 n_e^2 L \int_{-L}^{L} \left(M_L + \frac{R^2}{2r} \frac{dM_L}{dr} \right) d\zeta.$$

$$M_L = \frac{1}{3} b^2 \exp\left[-2r^2/(2l_B^2) \right] \Rightarrow M_k \propto k^4 \exp(-k^2 l_B^2/2).$$

For
$$L \gg l_B$$
, $C(R) = \frac{\sqrt{2\pi}}{3} K^2 n_e^2 L l_B \left(1 - \frac{R^2}{2l_B^2}\right) \exp\left(-\frac{R^2}{2l_B^2}\right)$.

$$C(R) \approx \frac{\sqrt{2\pi}}{3} K^2 n_e^2 L l_B \left(1 - \frac{R^2}{2l_B^2}\right) \exp\left(-\frac{R^2}{2l_B^2}\right).$$

The standard deviation of RM:

$$\sigma_{\mathrm{RM}}^2 = C(0) \quad \Rightarrow \quad \sigma_{\mathrm{RM}} \approx K n_e b \sqrt{L l_B}.$$

Interpretation: random walk of the polarization angle through N turbulent cells,

$$\sigma_{\psi} \propto \sqrt{N}, \quad N = L/l_B \implies \sigma_{\rm RM} \approx {\rm RM_0} \sqrt{N}, \quad {\rm RM_0} = K n_e b l_B.$$

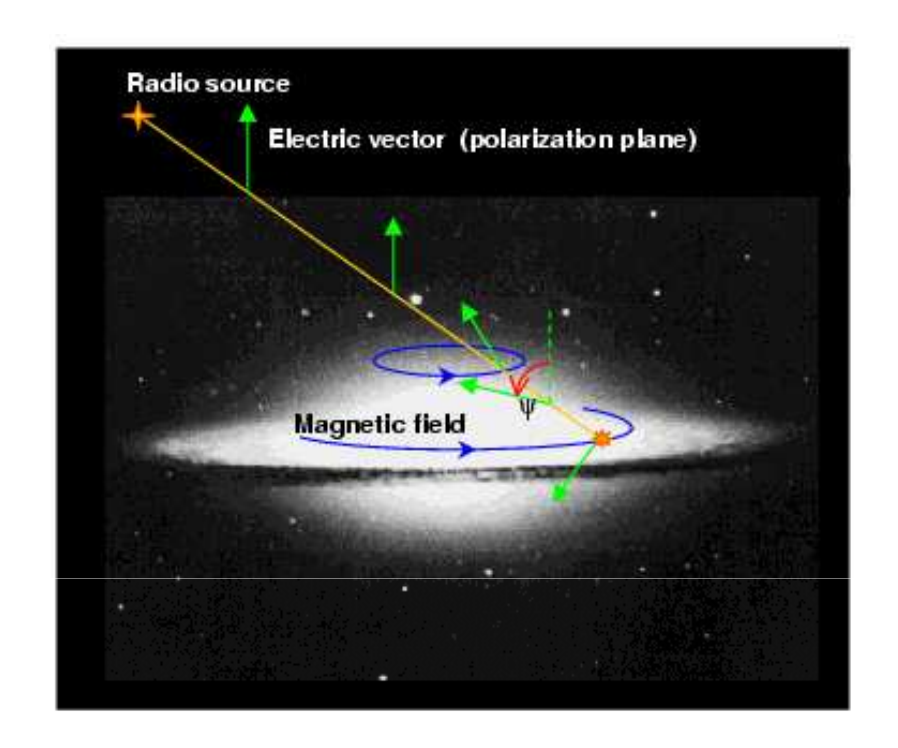
 ${
m RM}_0=$ Faraday rotation measure produced in a single turbulent cell, $l_B=$ magnetic turbulent scale, $n_e=$ thermal electron number density, b= the r.m.s. magnetic field, L= path length.

Interstellar medium

Faraday rotation of emission from external radio sources

or

of the intrinsic (galactic) synchrotron emission



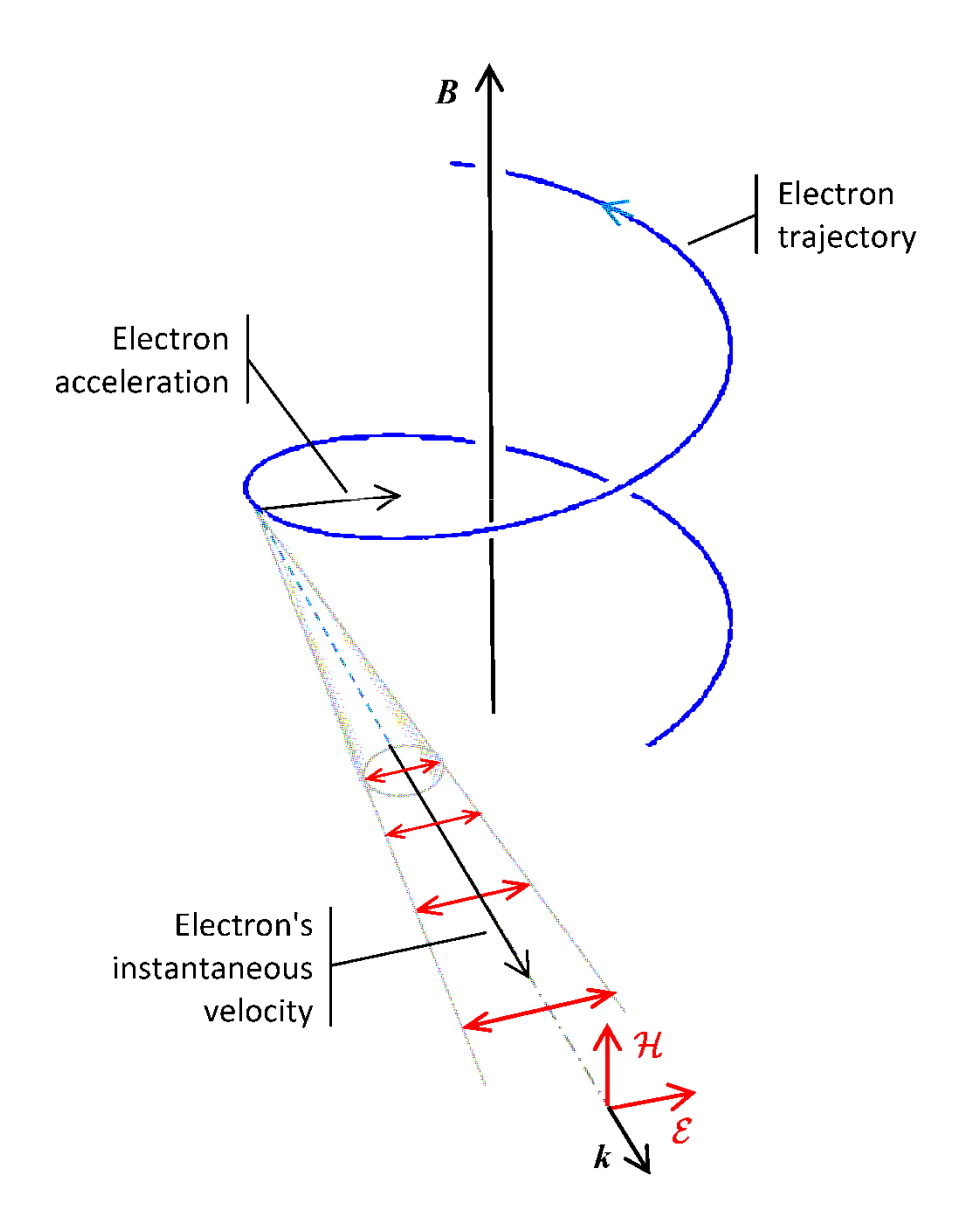
$$n_e = 0.03 \,\mathrm{cm}^{-3}, \quad B = 5 \times 10^{-6} \,\mathrm{G}, \quad L = 1 \,\mathrm{kpc}$$

$$\Rightarrow$$
 RM = 100 rad m⁻², $\Delta \psi = 200^{\circ}$ at $\lambda = 21$ cm.

(c) Synchrotron emission

Produced by a relativistic electron on gyrating in magnetic field

Linearly polarised in the orbit's plane (when observed in this plane)



Power-law energy spectrum of cosmic-ray electrons,

$$N_{c.r.}(E) dE = QE^{-s} dE, \qquad s \approx 2.7,$$

in $\vec{B} = \text{const}$ produces, at frequency ν , synchrotron emissivity

$$\epsilon(\nu) = a(s) \frac{e^3 B_{\perp}}{mc^2} Q \left(\frac{3e B_{\perp}}{4\pi m^3 c^5} \nu^{-1} \right)^{(s-1)/2} \left[\frac{\text{erg}}{\text{s cm}^3 \text{Hz}} \right],$$

with the degree of polarisation

$$p_0 = \frac{s+1}{s+7/3} \approx 0.74.$$

Total intensity of of synchrotron emission ($\vec{s} = \text{line of sight}$)

$$I(\nu) = \int_0^L \epsilon(\nu) \, ds \propto \int_0^L n_{c.r.} B_{\perp}^2 \, ds.$$

In a partially ordered magnetic field,

$$\vec{B} = \vec{B}_0 + \vec{b}, \ \langle \vec{B} \rangle = \vec{B}_0, \ \langle \vec{b} \rangle = 0 \ \Rightarrow \ I = P(\vec{B}_0) + \text{unpolarised}(\vec{b}).$$

polarised synchrotron emission (intensity P) traces the large-scale magnetic field:

$$P(\nu) = p_0 \int_0^L \epsilon(\nu) \exp[2i(\psi_0 + RM(s)\lambda^2)] ds \propto \int_0^L n_{c.r.} B_{0\perp}^2 ds.$$

Assuming energy equipartition between cosmic rays & magnetic fields,

$$n_{c.r.} \propto B^2$$

 B_{\perp} and $B_{0\perp}$ can be determined from synchrotron observations.

Unpolarised part, I - P: tracer of the turbulent magnetic field.

Fractional polarisation:

$$p=rac{P}{I}pproxrac{B_{0\perp}^2}{\langle B_{\perp}^2
angle}=p_0rac{B_{0\perp}^2}{B_{0\perp}^2+rac{2}{3}\langle b^2
angle}\;.$$

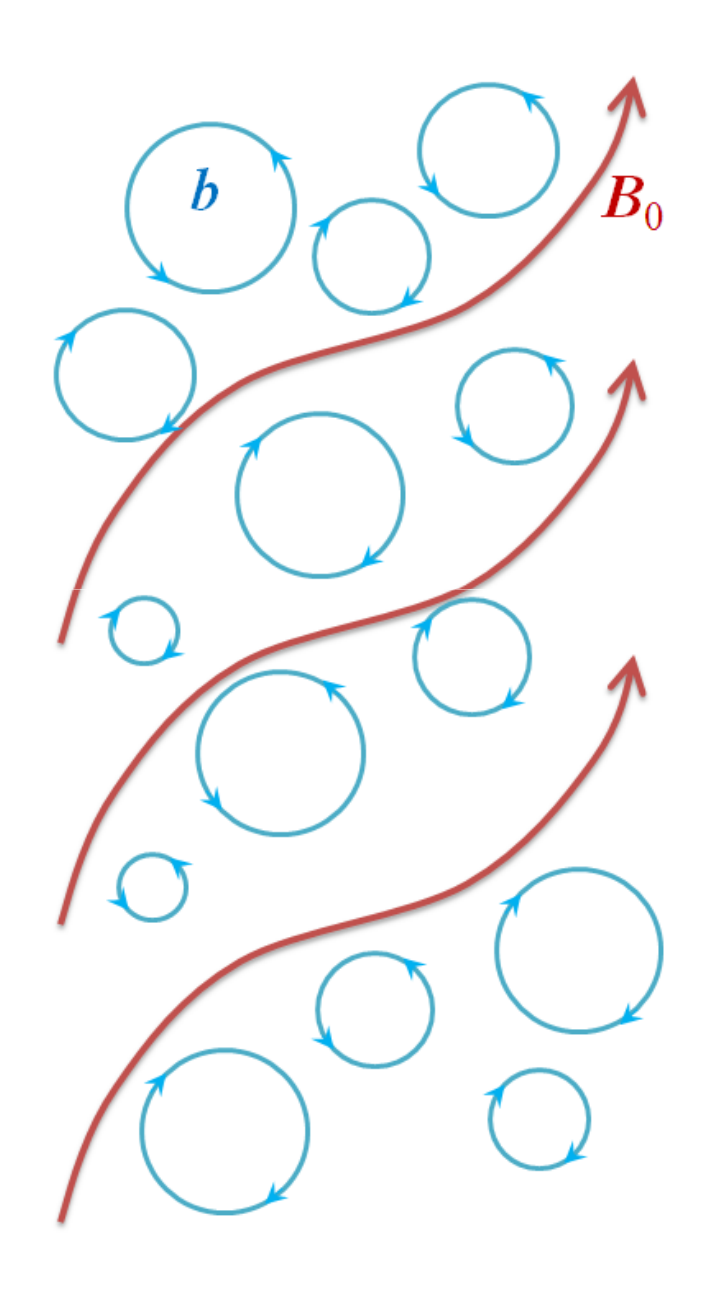
(for an *isotropic* random field)

$$I, P \Rightarrow B_{0\perp}, b, \text{ given } n_{\text{c.r.}}$$

(most often, energy equipartition or pressure balance)

Faraday rotation and synchrotron emission provide the most important observational methods for galactic and extragalactic magnetic fields

Synchrotron polarization in isotropic magnetic field



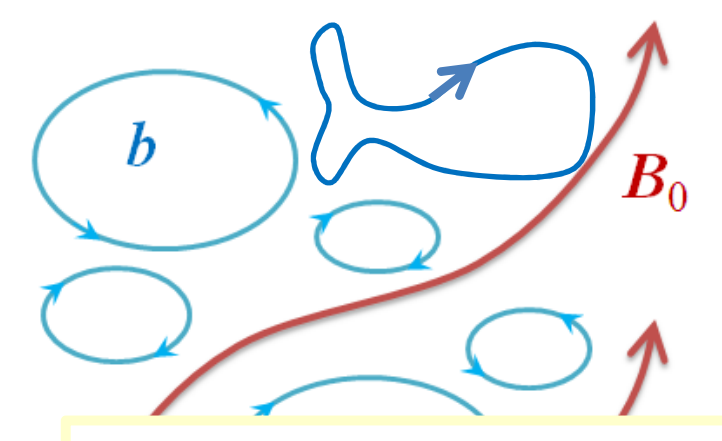
All polarized emission produced by the large-scale magnetic field. Fractional polarization:

$$p = \frac{P}{I} = p_0 \frac{B_{0x}^2 + B_{0y}^2}{B_{0x}^2 + B_{0y}^2 + \frac{2}{3}b^2} .$$

But Faraday rotation is due to the large-scale field alone:

$$RM = K n_e B_{0z} L$$
.

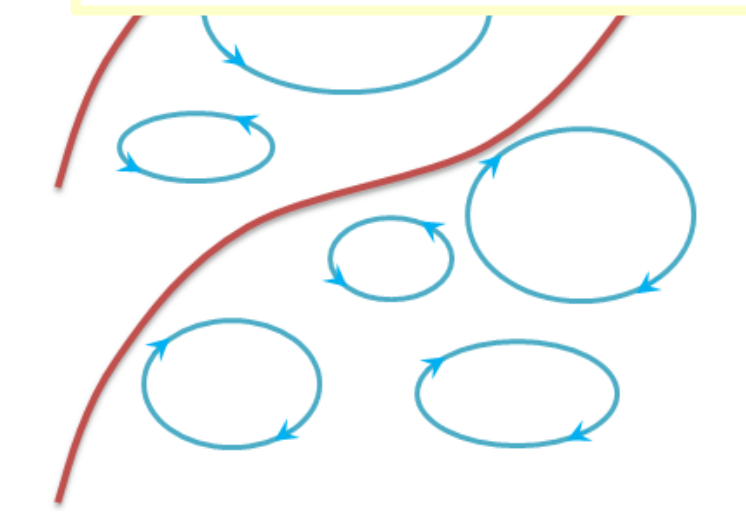
Synchrotron polarization in anisotropic magnetic field



Anisotropic random field also produces polarized synchrotron emission.

Fractional polarization (Sokoloff et al., 1998):

$$p = \frac{P}{I} = p_0 \frac{\left[\left(B_{0x}^2 - B_{0y}^2 + b_x^2 - b_y^2 \right)^2 + 4B_{0x}^2 B_{0y}^2 \right]^{1/2}}{B_{0x}^2 + B_{0y}^2 + b_x^2 + b_y^2}$$

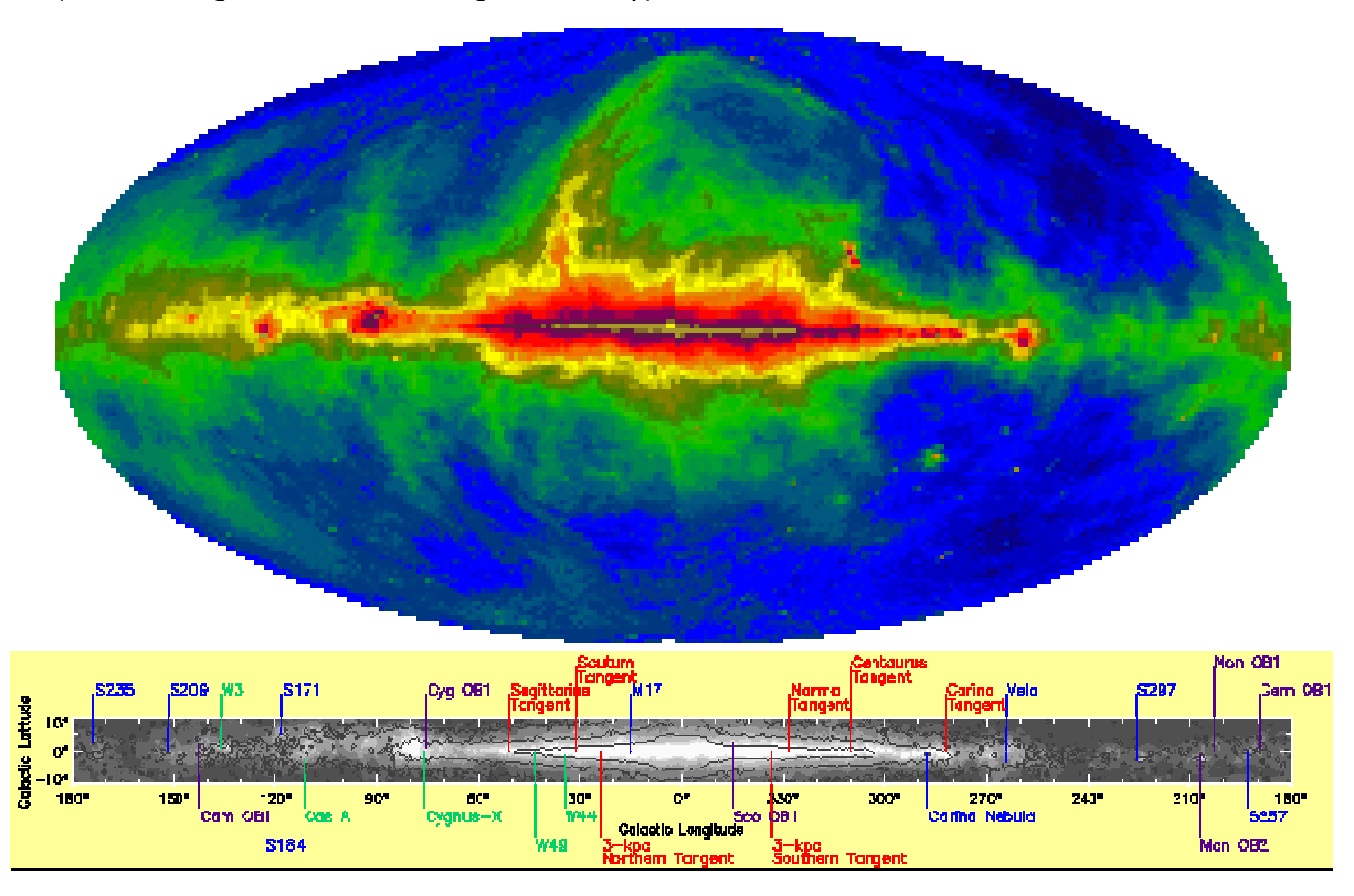


But Faraday rotation is due to the large-scale field alone:

$$RM = K n_e B_{0z} L$$
.

Milky Way, I at v = 408 MHz ($\lambda = 73.5$ cm)

(100-m single dish, Effelsberg, Germany)



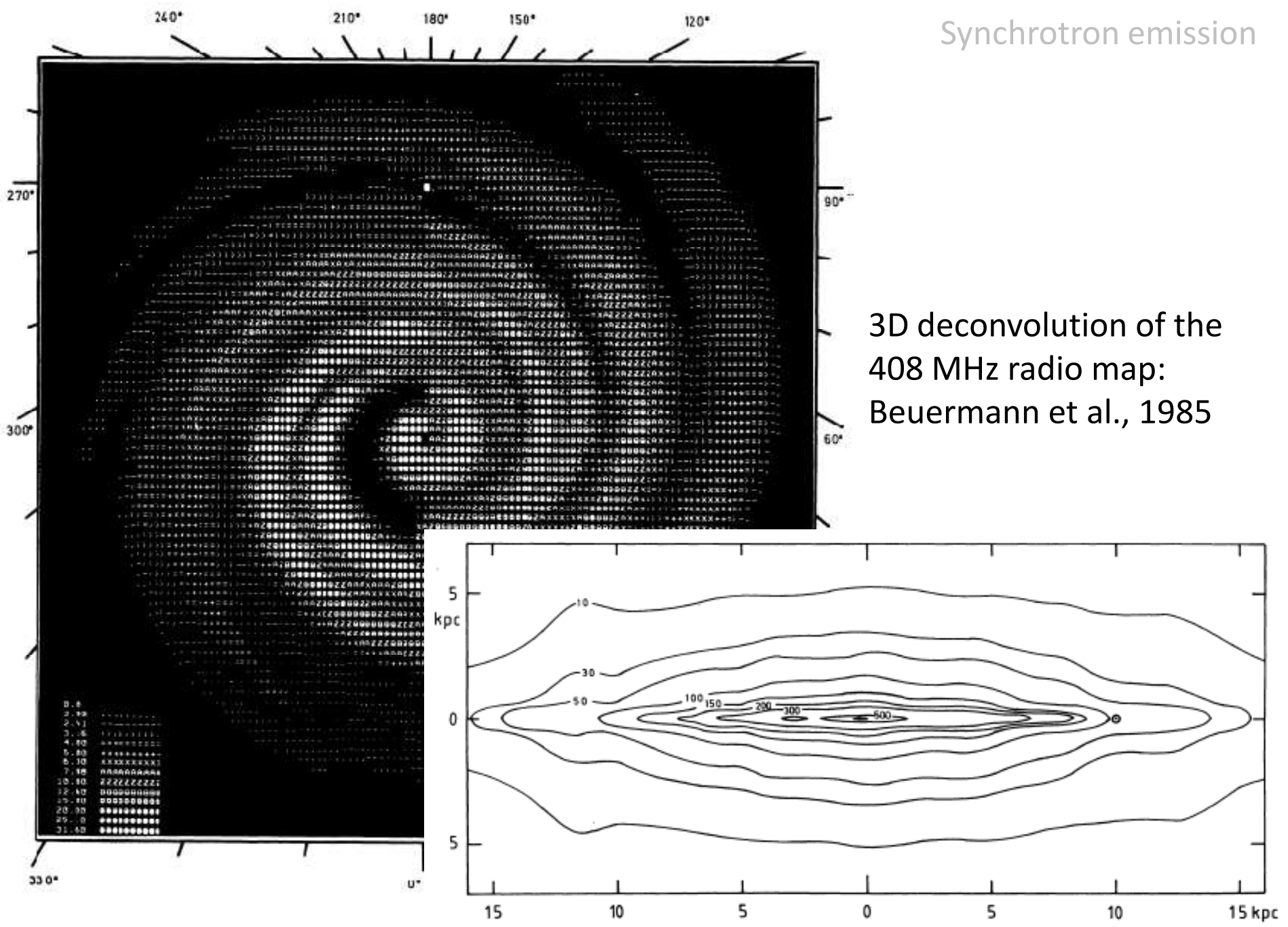
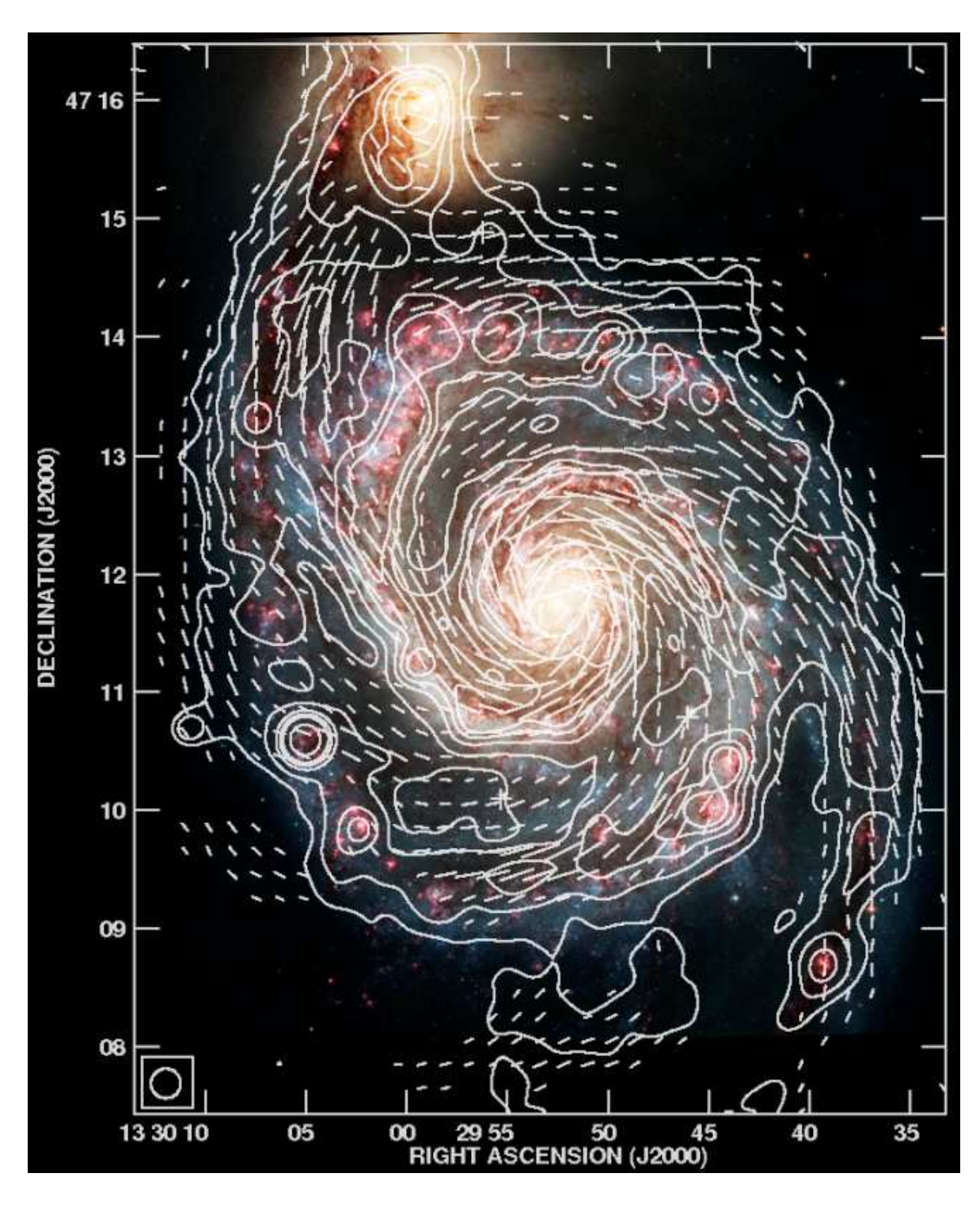


Fig. 9. Edge-on view of the Galaxy at 408 MHz as seen from the direction $l = 90^\circ$. The picture includes the emission from the thin and the thick disk. The contour intervals are given in degree K. For comparison with external galaxies note that the 30-K level corresponds to about 1 K at 1415 MHz for a flux-density spectral index a = 0.8



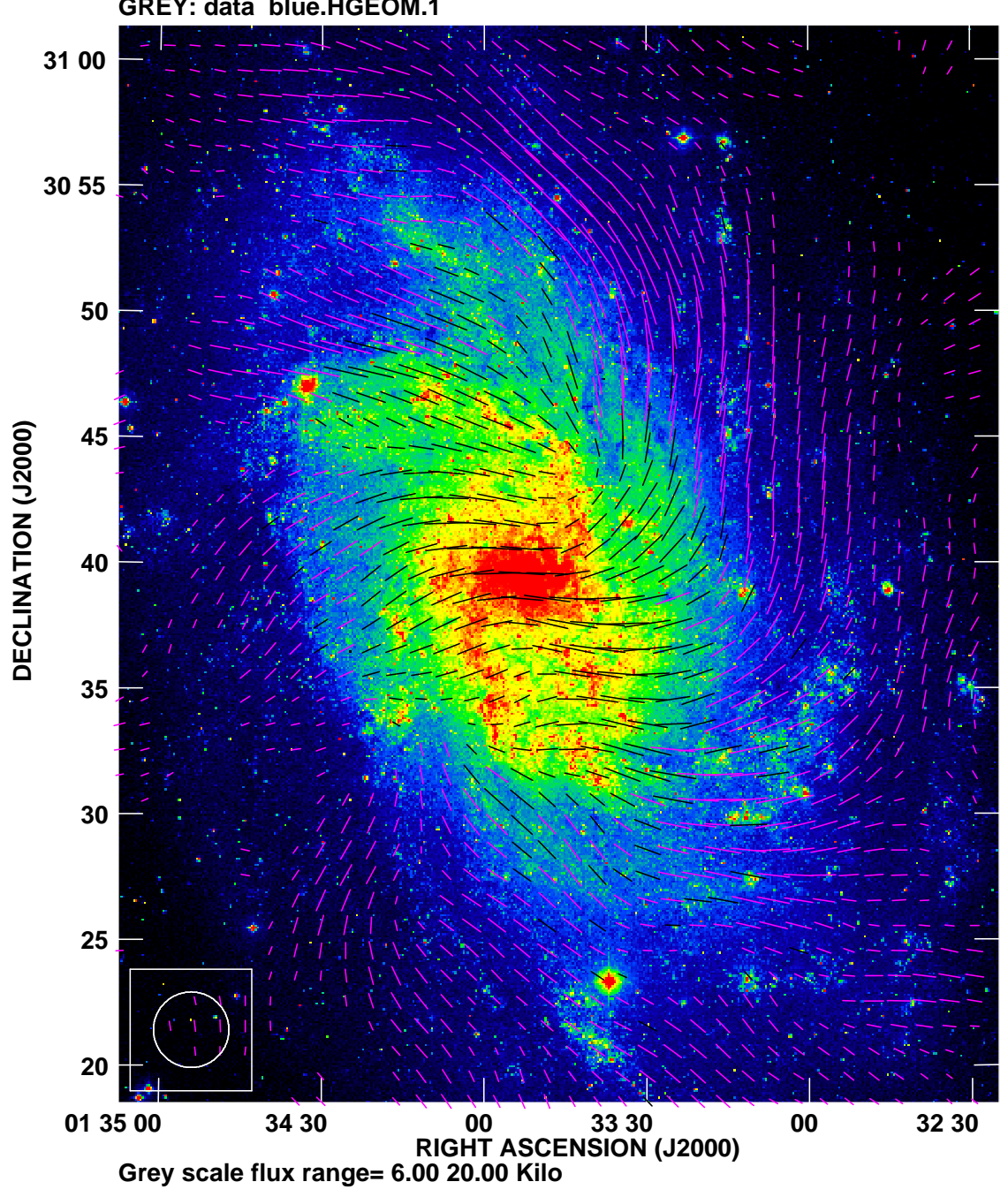
M51:

pprox face-on, $i=22^{\rm o}$, at $\lambda 6$ cm

I-contours + *B*-vectors

(Effelsberg+VLA;

A. Fletcher & R. Beck)



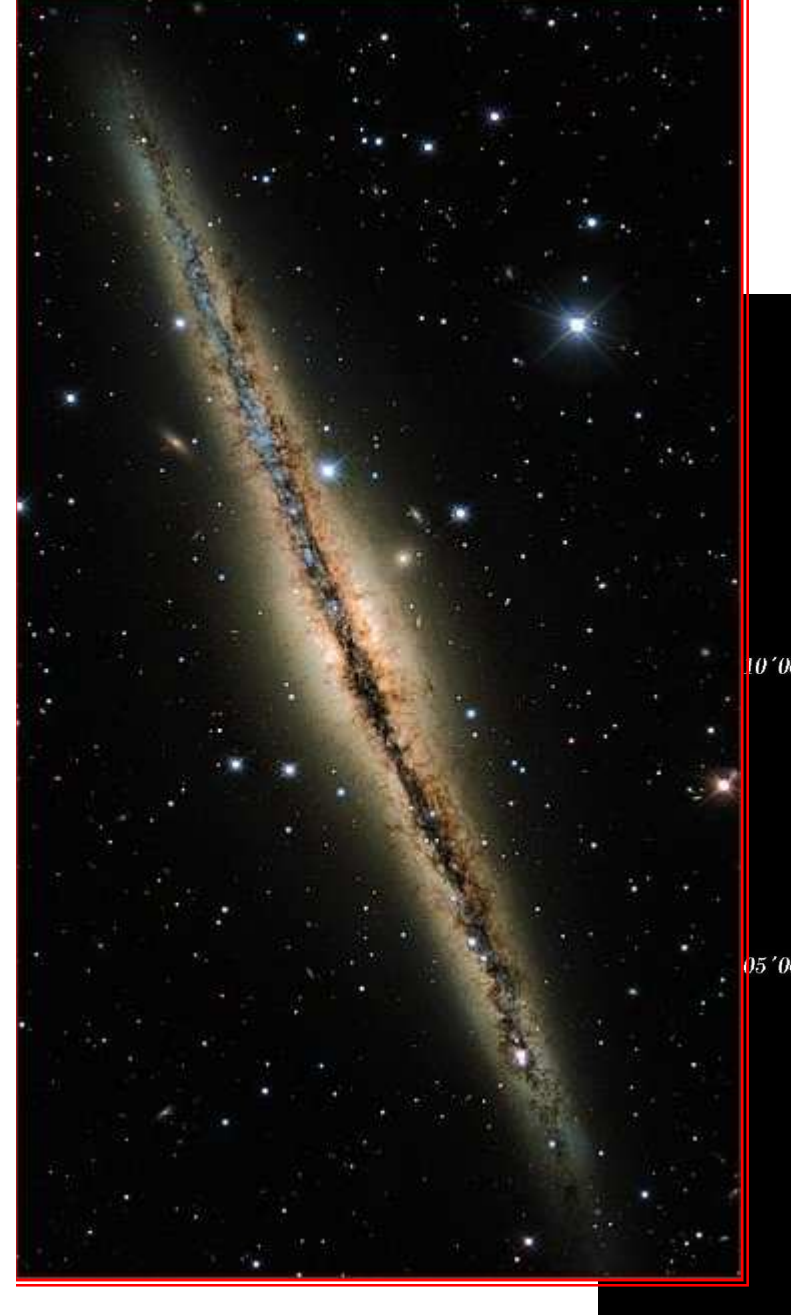
M33:

 $i=52^{\rm o}$, at $\lambda 3.6$ cm

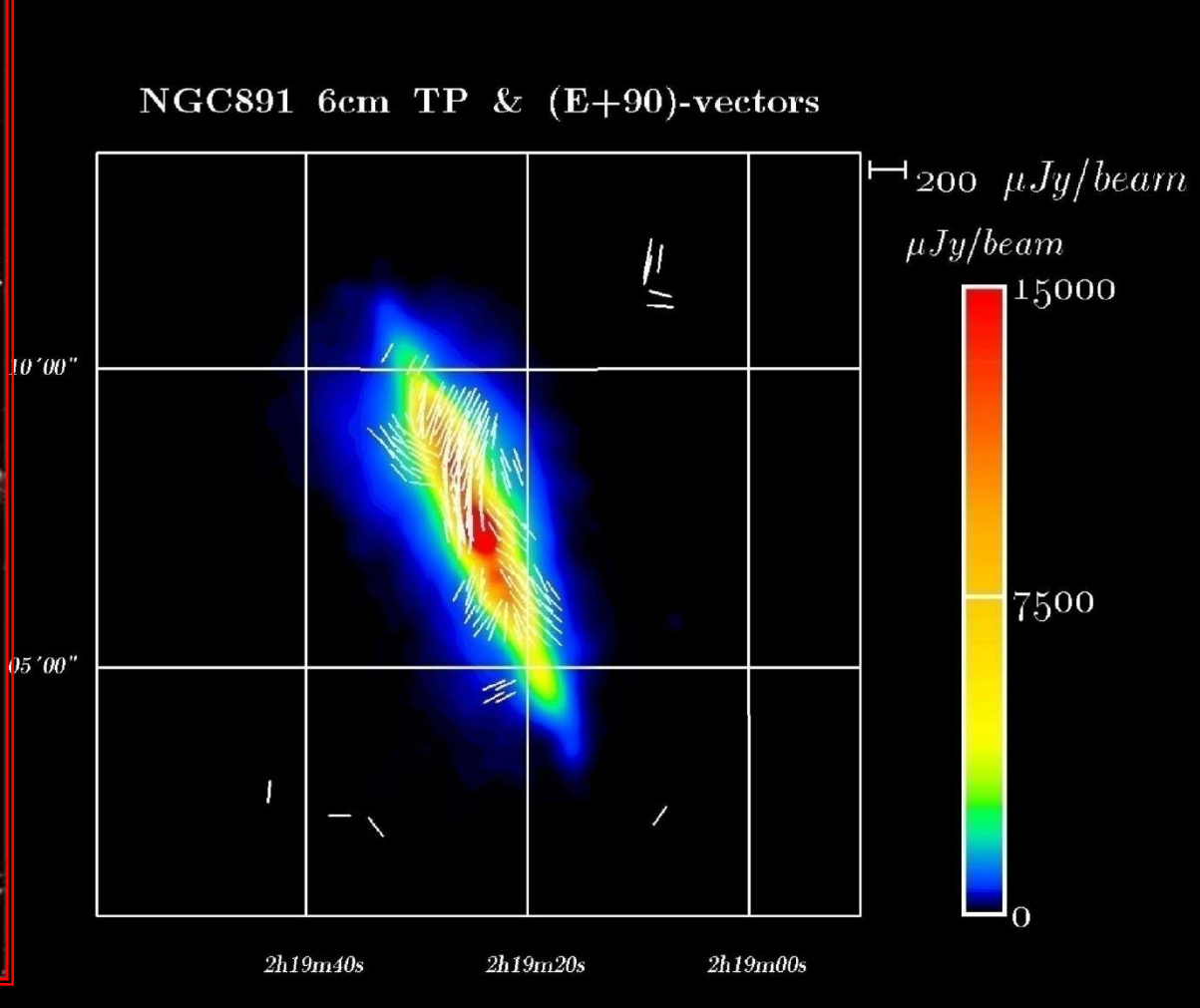
B-vectors

(Effelsberg+VLA;

F. Tabatabaei & R. Beck)



NGC 891: a galaxy visible edge-on, $i = 89^{\circ}$

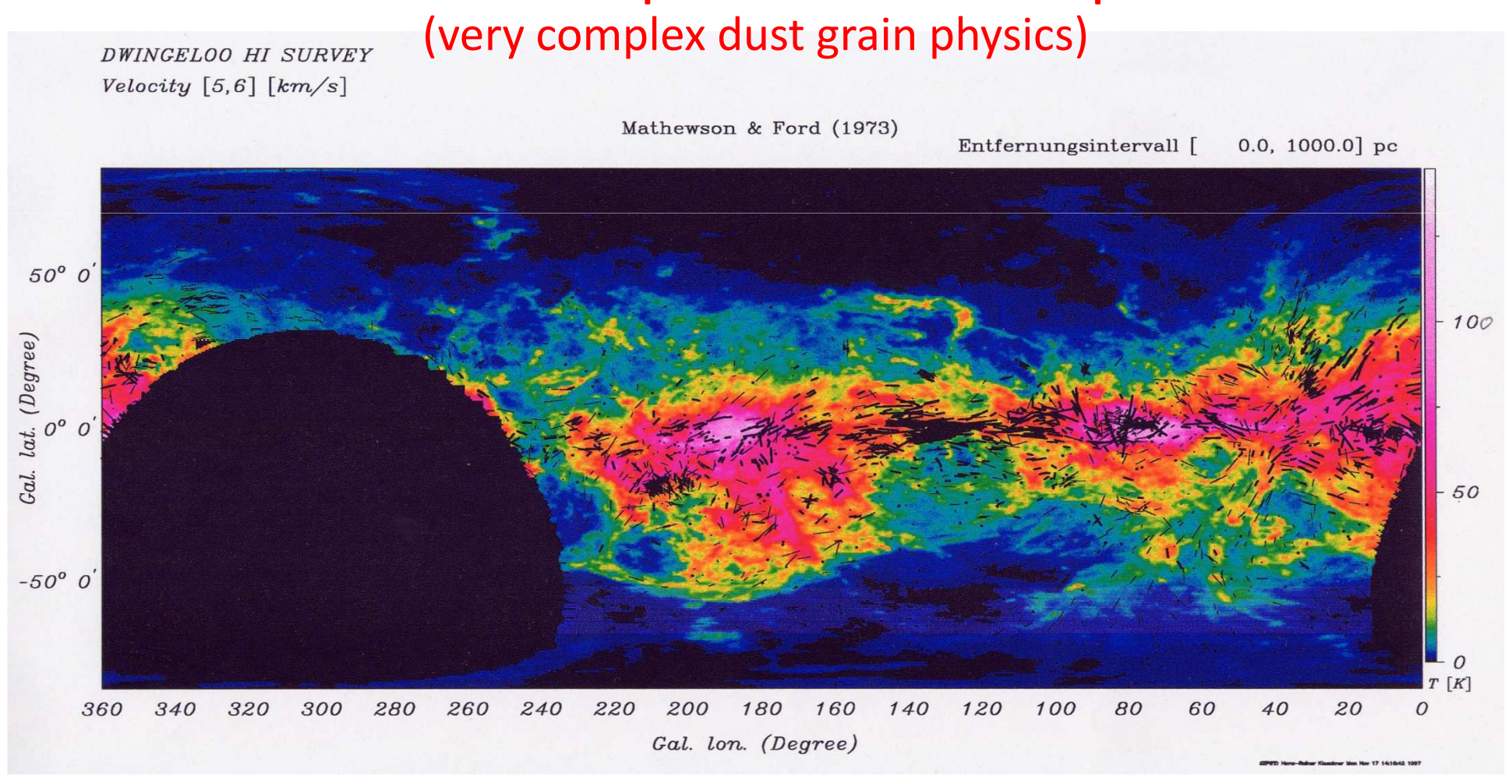


MPIfR, Bonn

(d) Light polarisation by dust

Non-spherical dust grains aligned by magnetic field ⇒selective absorption ⇒ polarised starlight

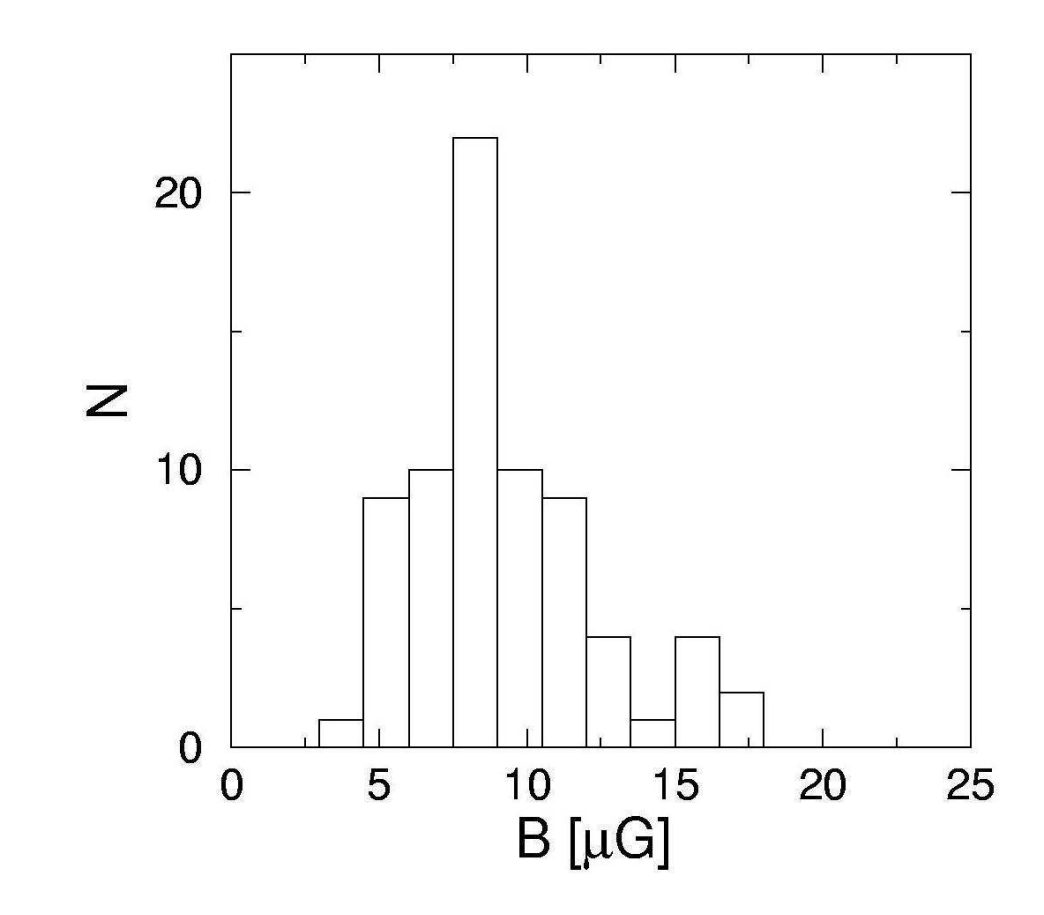
No solid basis for quantitative interpretations



2. Galactic and extragalactic magnetic fields from observations

2.1. Spiral galaxies

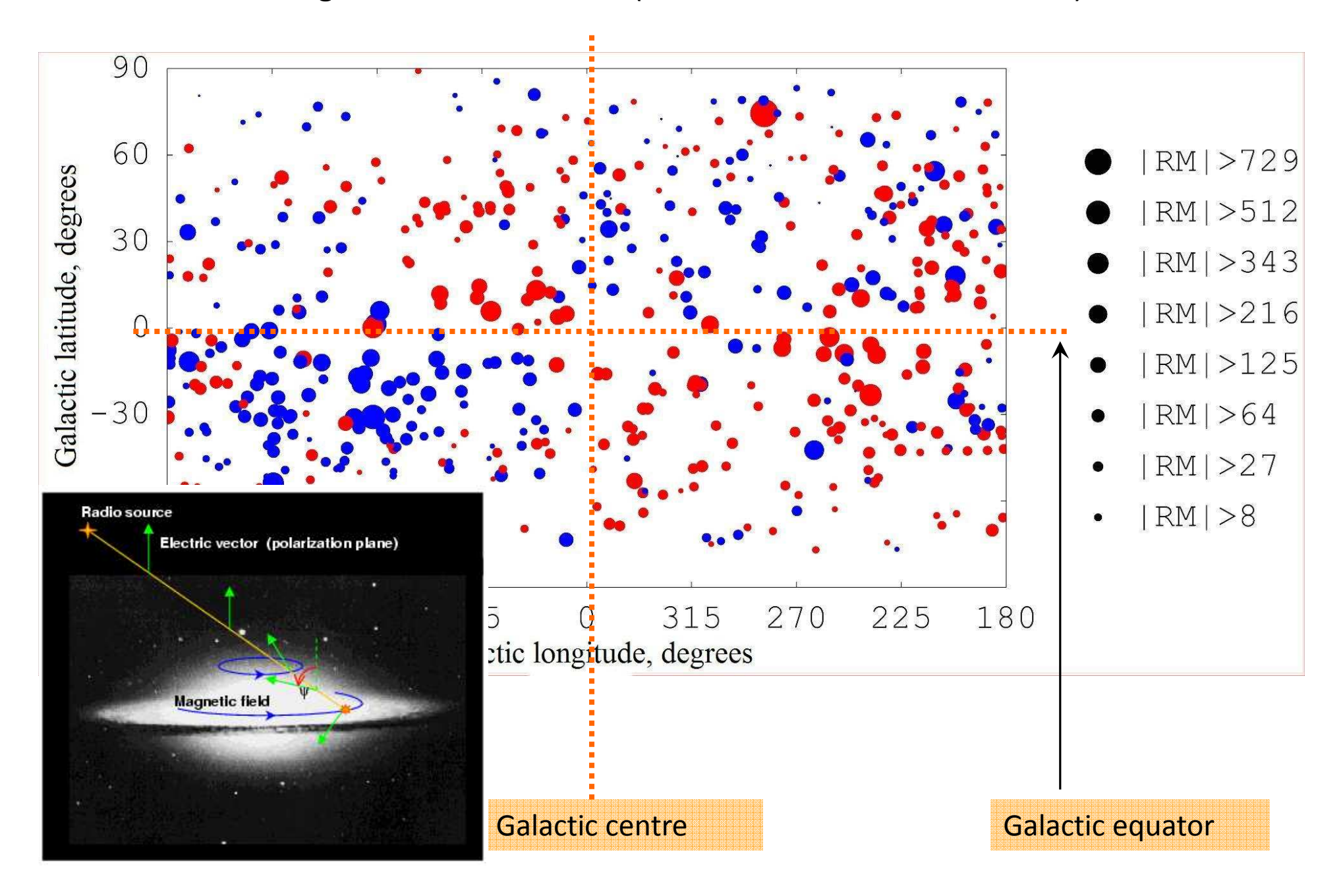
$$B = 5 - 12 \,\mu\text{G}$$



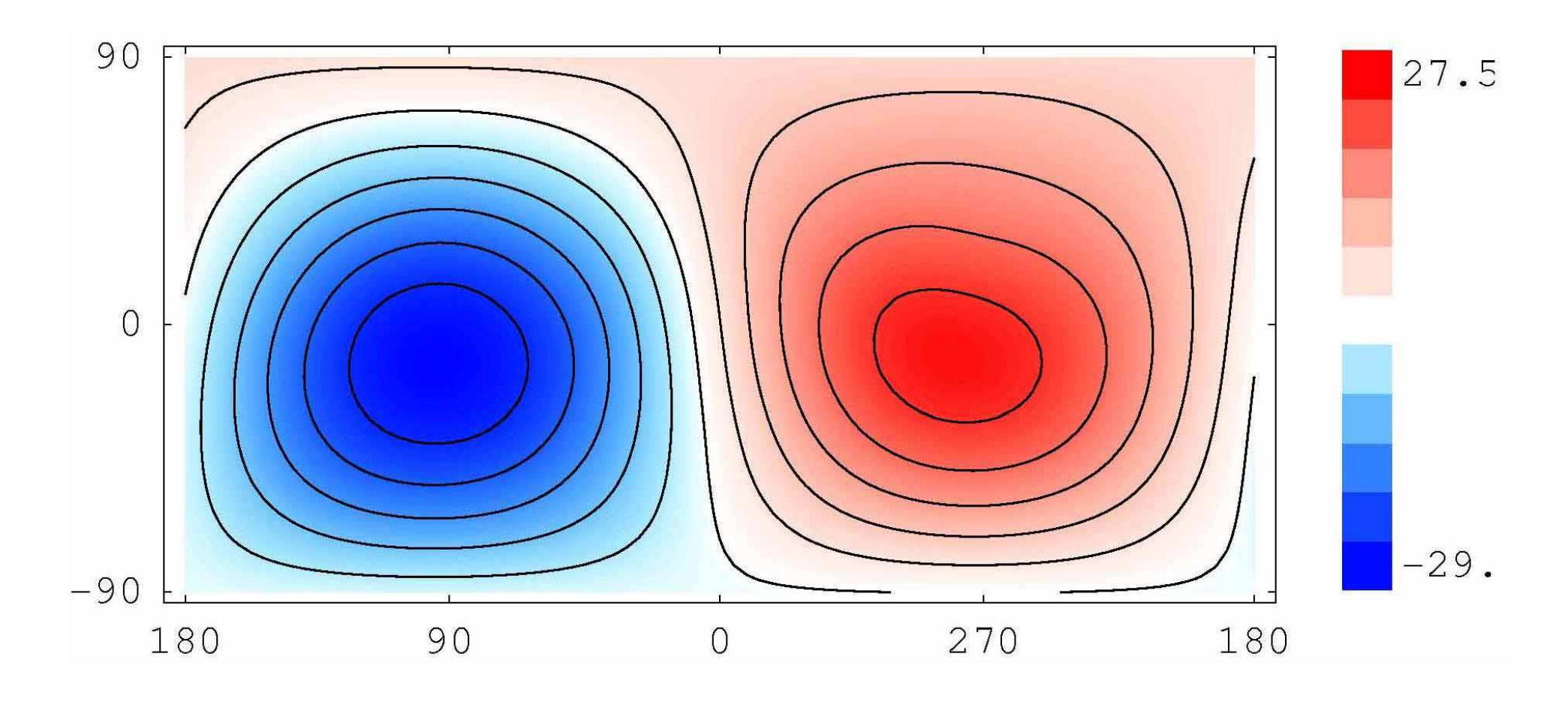
Histogram of total magnetic field strengths in a sample of spiral galaxies (assuming equipartition between cosmic rays and magnetic fields) (Niklas 1995)

Magnetic field in the Milky Way

RMs of 674 extragalactic radio sources (Simard-Normandin et al. 1981)



Wavelet transform, max-power scale 76° (Frick et al. 2001)

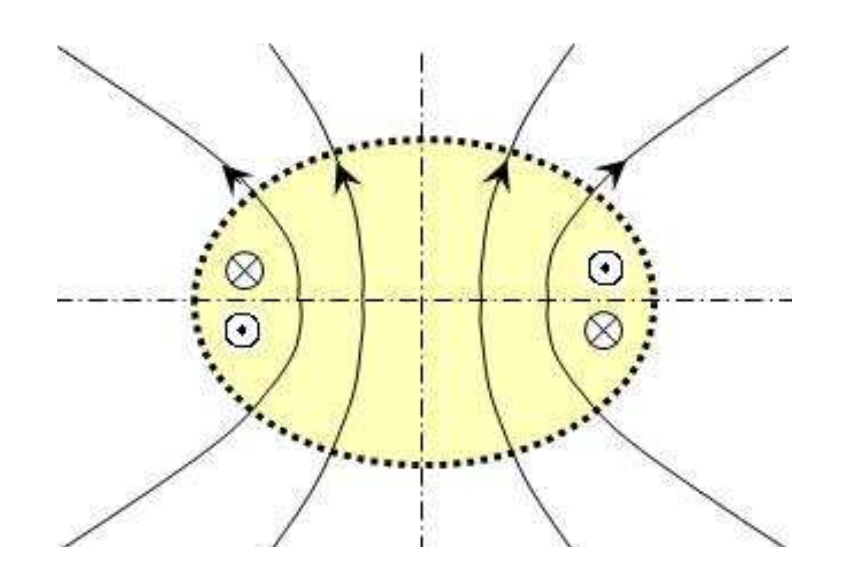


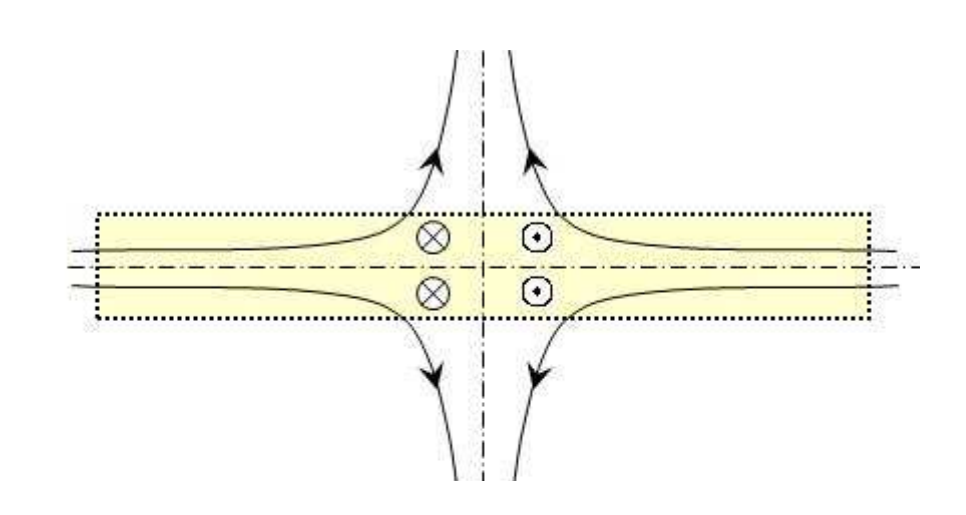
Quadrupolar symmetry:

$$B_{\phi}(z) = B_{\phi}(-z), \ B_{r}(z) = B_{r}(-z), \ B_{z}(z) = -B_{z}(-z)$$

Dipolar symmetry (quasispherical objects)

Quadrupolar symmetry (flat objects)

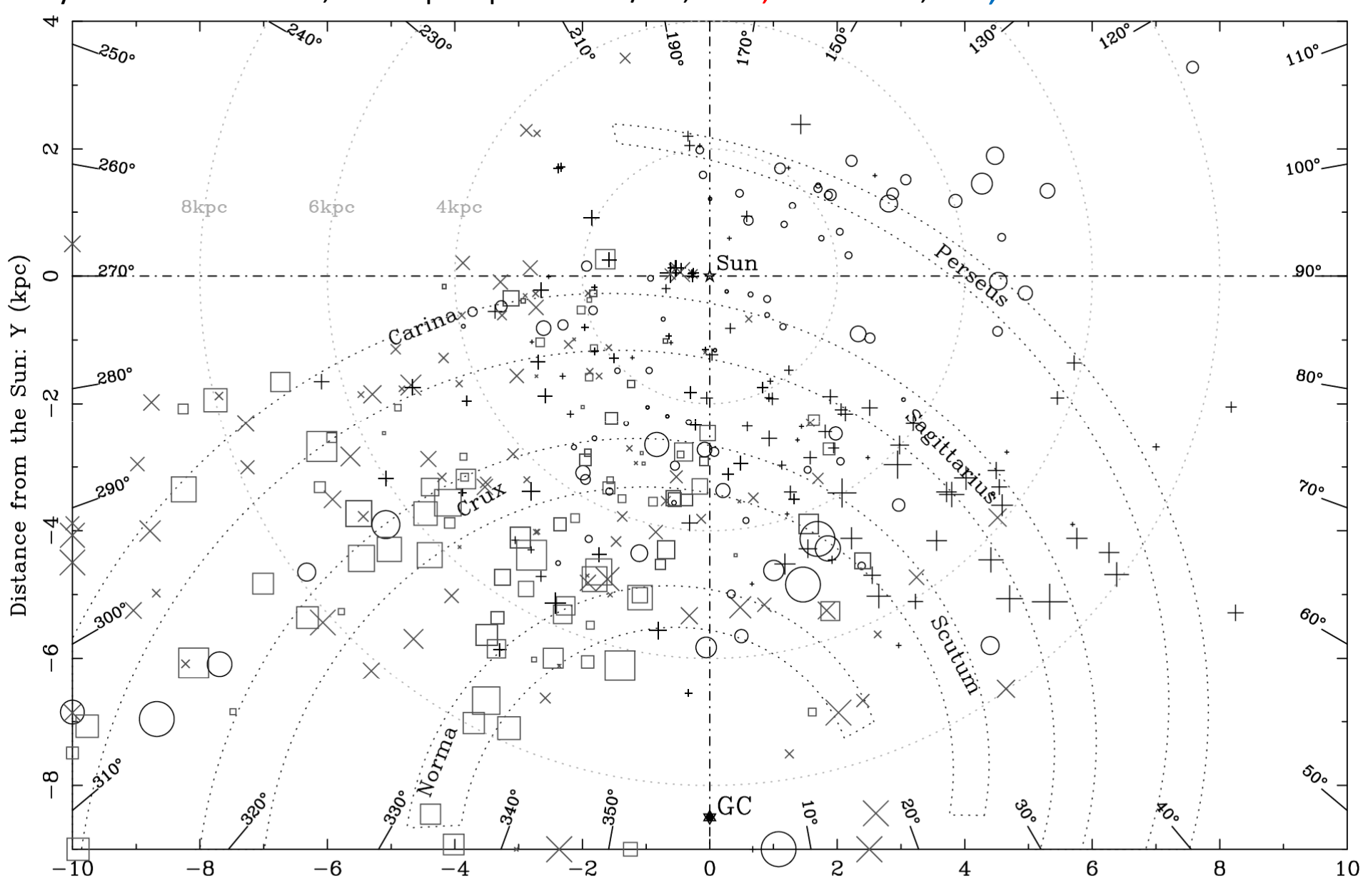




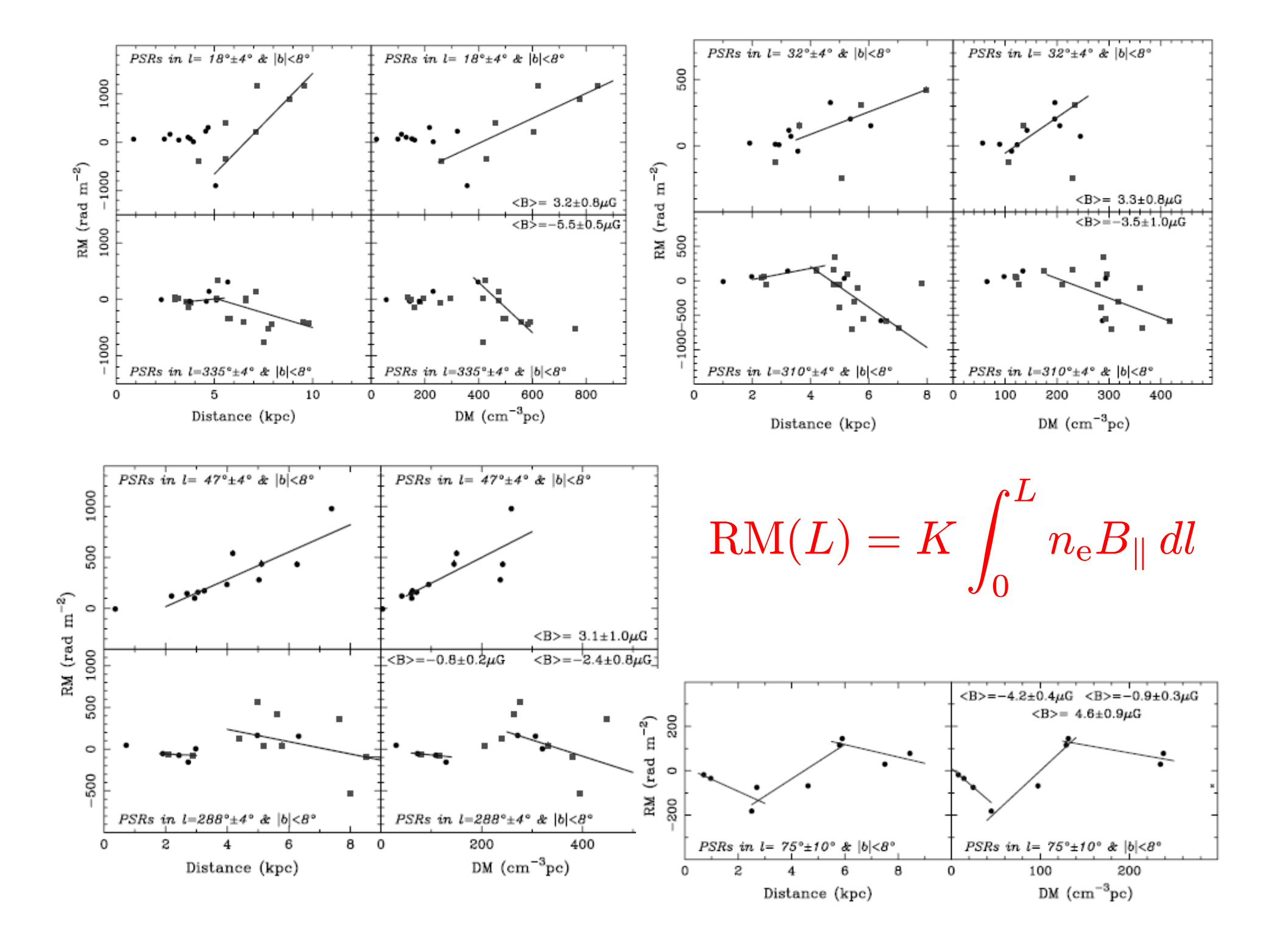
Decay times:

$$au_{
m dipole} \simeq (h/2)^2 \eta^{-1}$$
 $au_{
m quadrupole} \simeq h^2 \eta^{-1}$
 $au_{
m dipole} \approx \frac{1}{4} au_{
m quadrupole}$

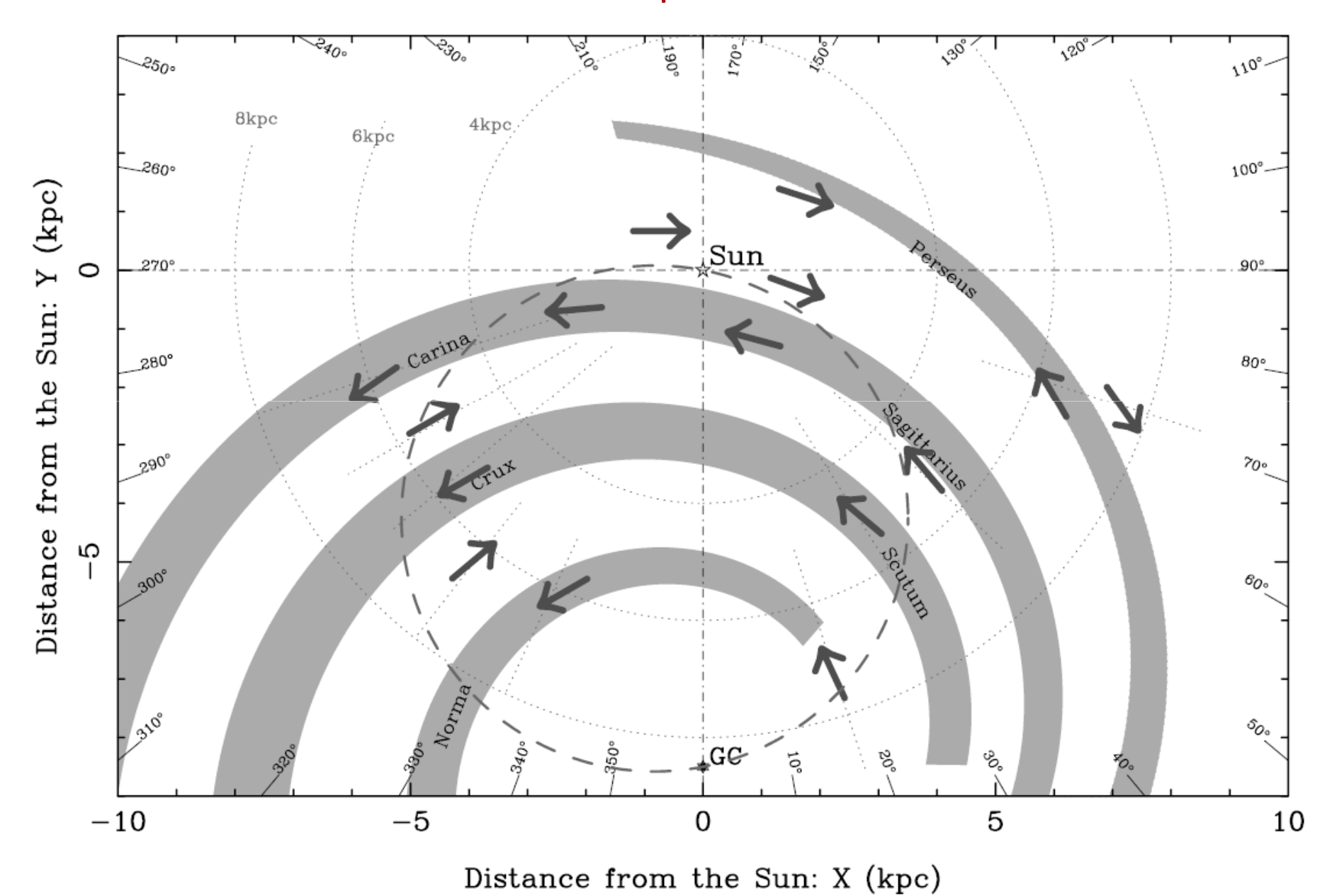
RMs of 388 pulsars with $|b| < 8^{\circ}$, projected onto the Galactic plane (Han et al., 2006), symbol size $\propto RM^{1/2}$, $9 < |RM| < 900 \text{ rad/m}^2$, $+, \times : RM > 0$, \bigcirc , $\square : RM < 0$.



Distance from the Sun: X (kpc)

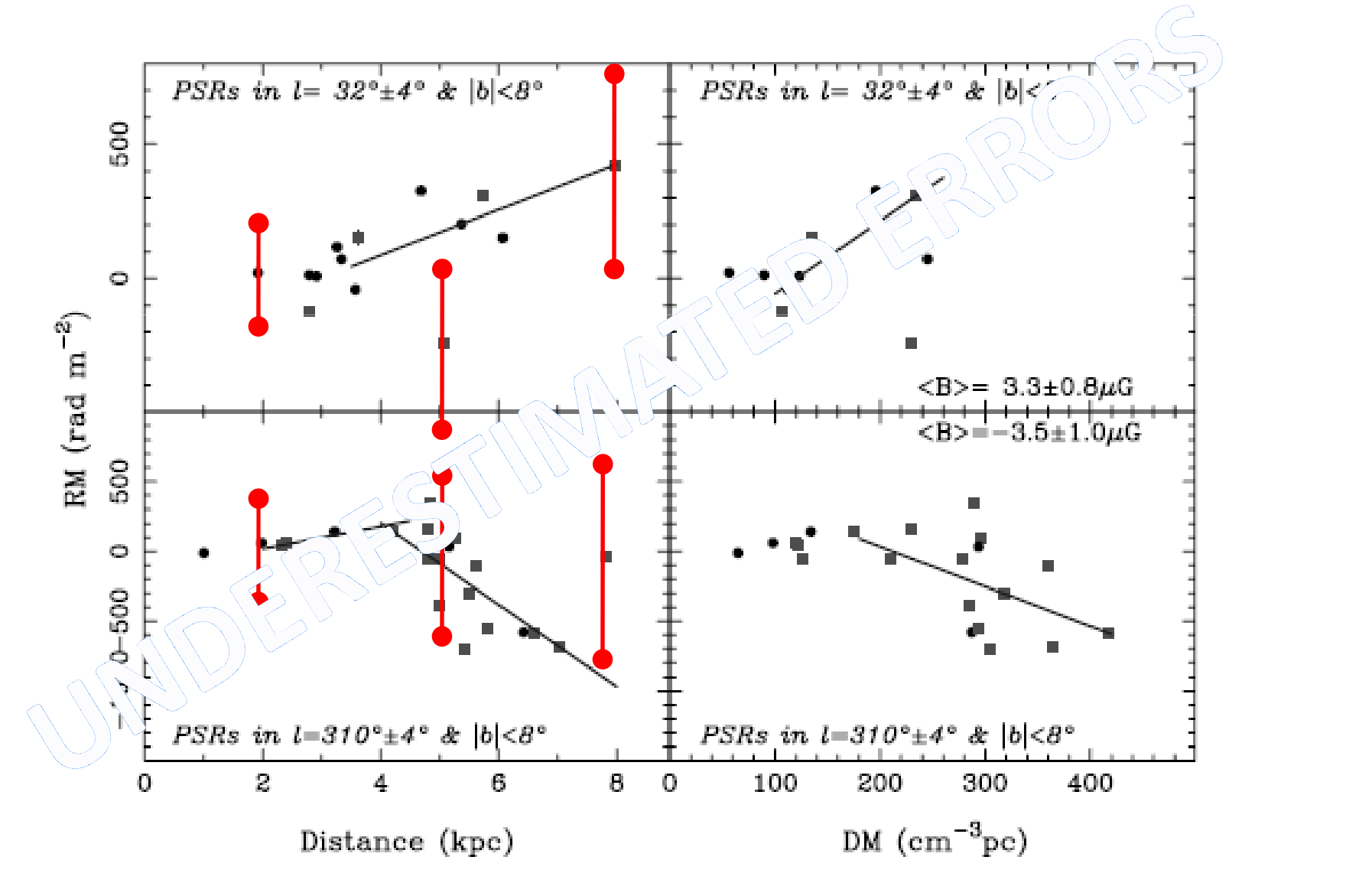


Fit to RMs of 388 pulsars with |b| < 8° (Han et al., 2006): overinterpretation.

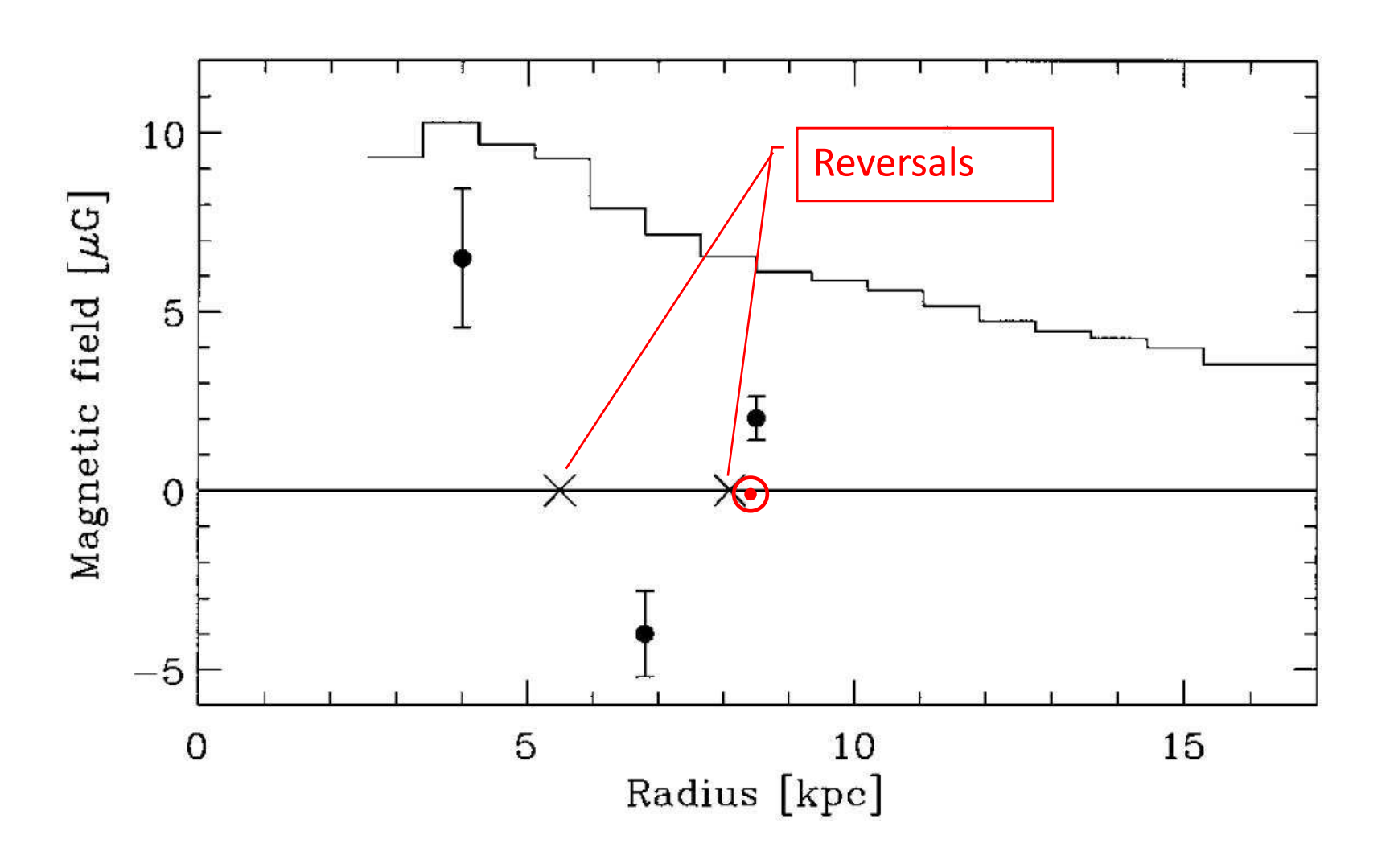


$$\sigma_{\mathrm{RM}} = 2\sqrt{n_{\mathrm{e}}bdL}$$

$$= 250 \,\mathrm{rad} \,\mathrm{m}^{-2} \left(\frac{n_{\mathrm{e}}}{0.03 \,\mathrm{cm}^{-3}}\right)^{1/2} \left(\frac{b}{5 \,\mu\mathrm{G}}\right)^{1/2} \left(\frac{d}{100 \,\mathrm{pc}}\right)^{1/2} \left(\frac{L}{1 \,\mathrm{kpc}}\right)^{1/2}$$

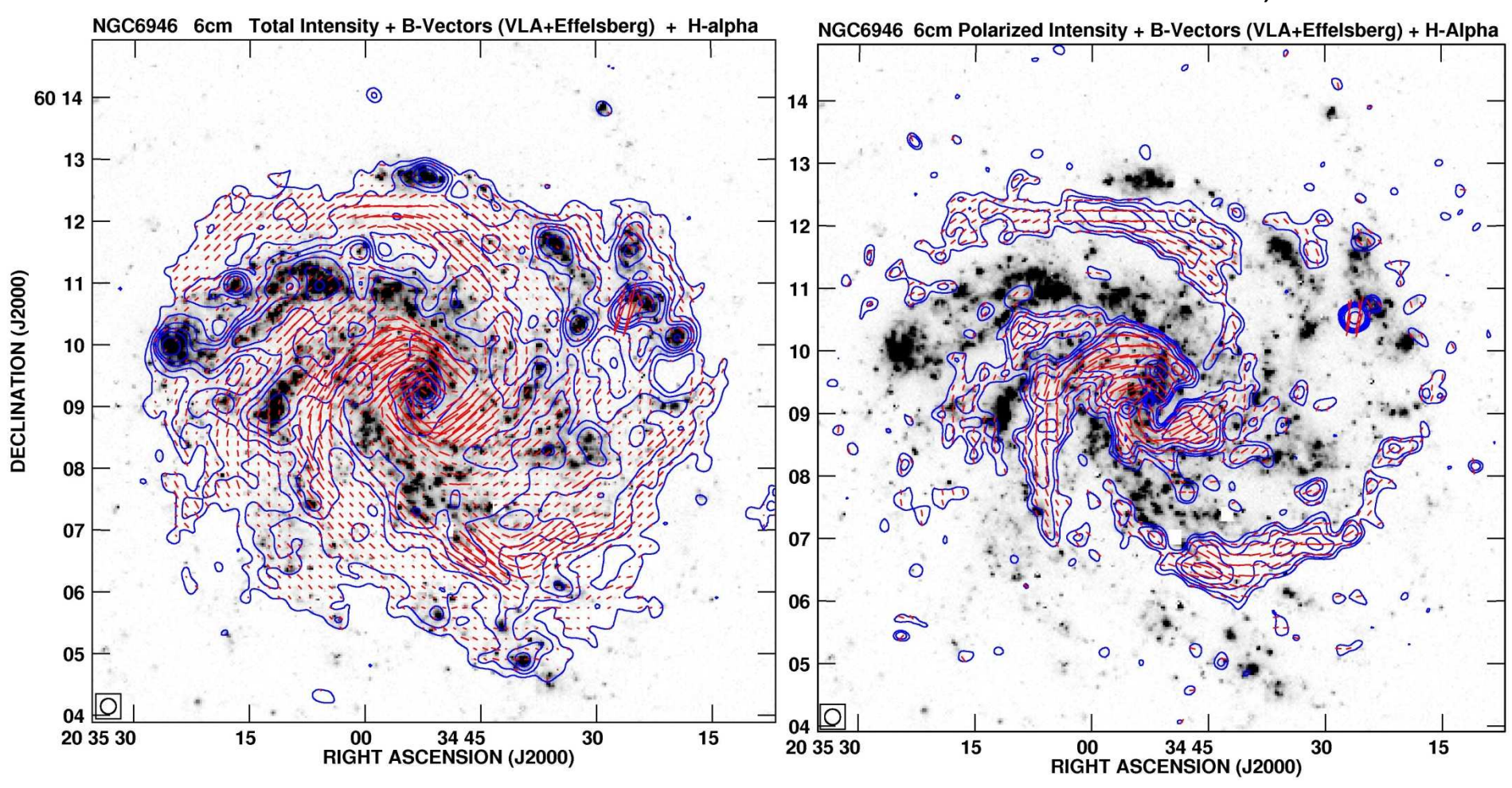


Total and regular magnetic fields in the Milky Way



NGC 6946: magnetic arms

R. Beck, A&A 2007



Large-scale magnetic field is stronger between the spiral arms, where gas density is lower: it is not frozen into the gas!

M51: distinct magnetic fields in the disc and halo

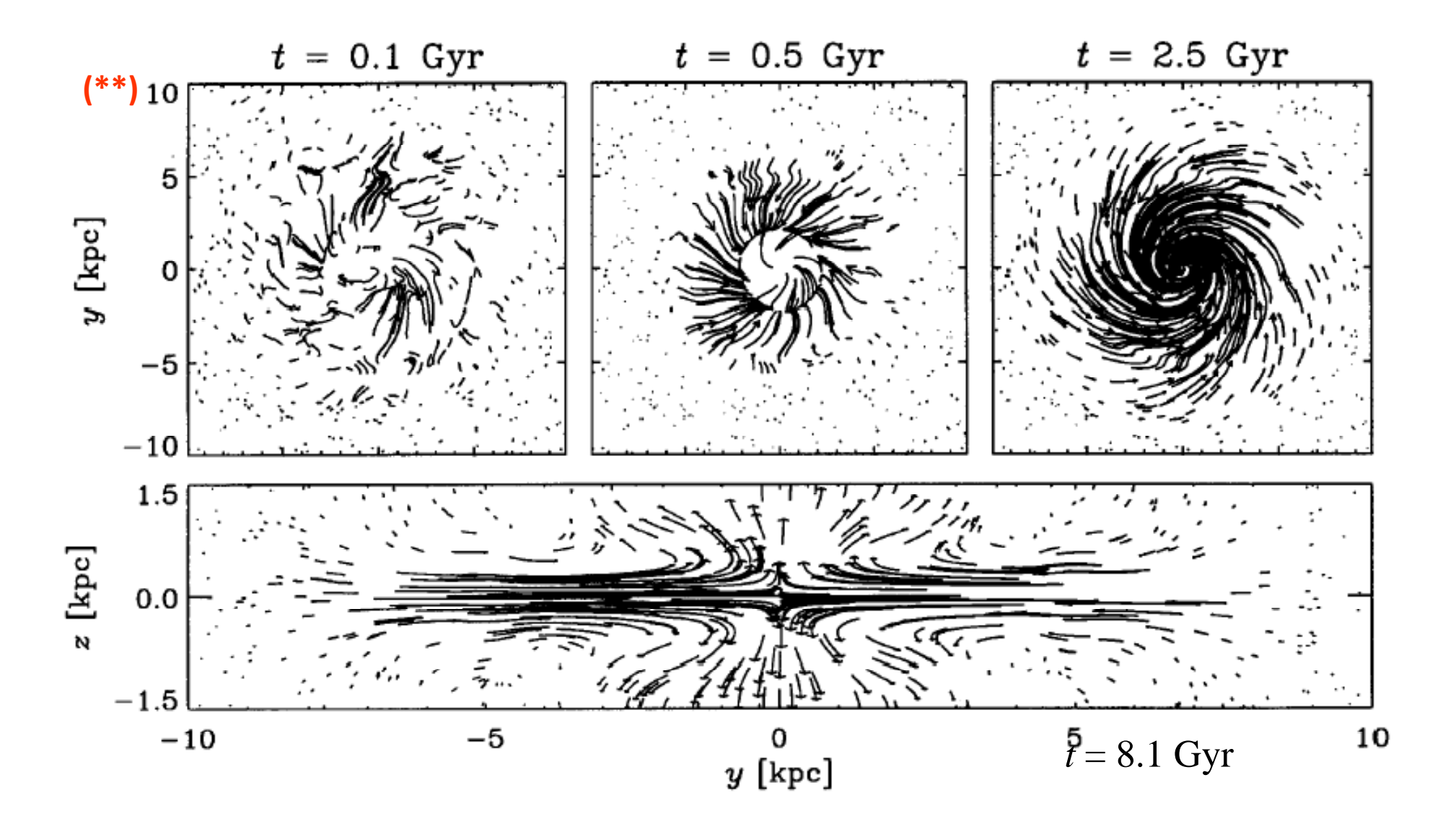
Fletcher et al., 2010



Large-scale magnetic fields in the disc and halo have different symmetries!

Magnetic fields in spiral galaxies: summary

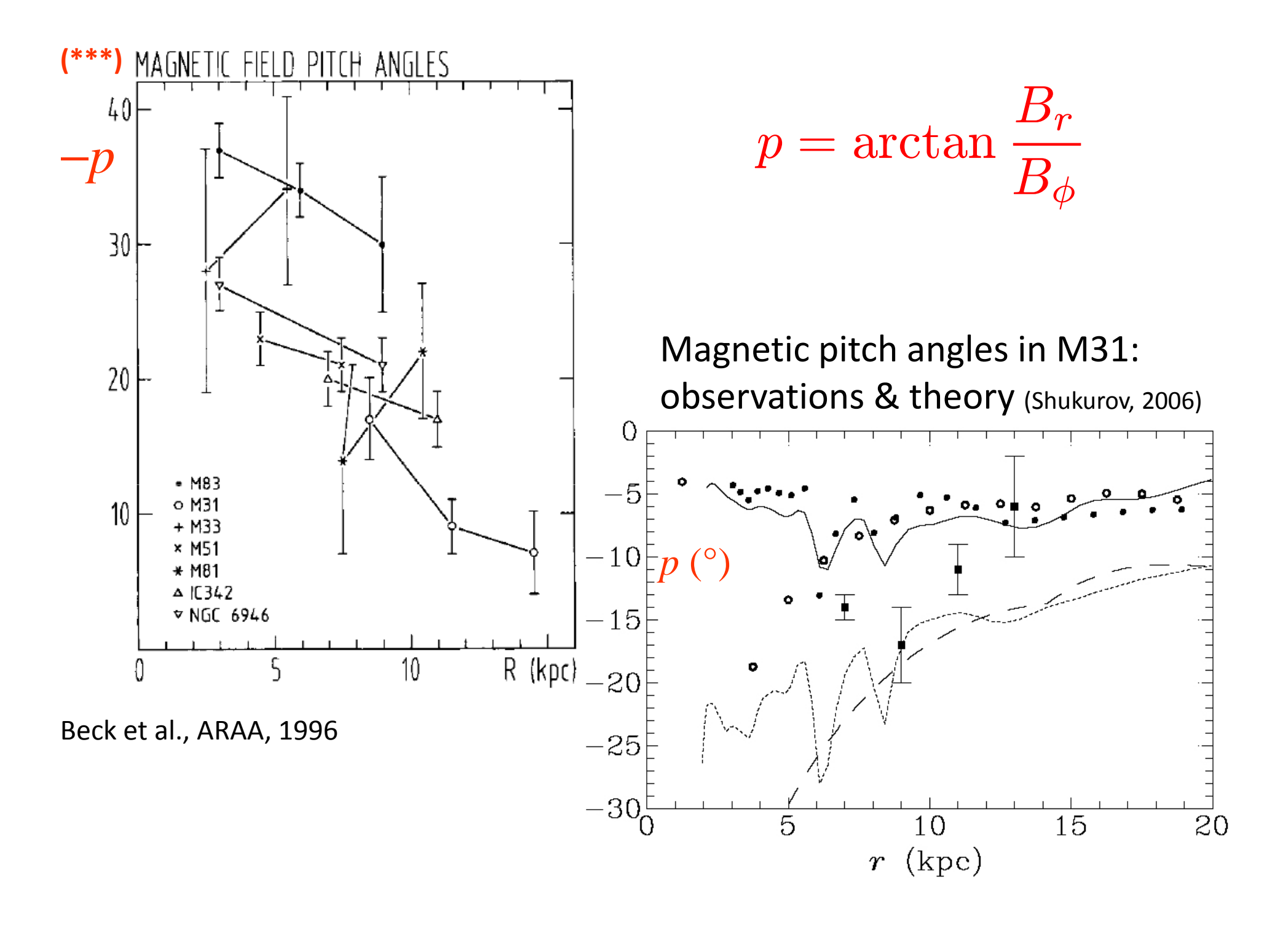
- $\square B = 5-12 \ \mu G$, $B_0 = 3-7 \ \mu G$, $b^2/B_0^2 = 3$, approximate equipartition with turbulent energy, $b \cong (4\pi\rho)^{1/2} \ v_0 \simeq 5 \ \mu G$
- ☐ Quadrupolar global parity (**)
- Overall trailing spiral pattern, $\arctan B_{\gamma}/B_{\phi} = -(10^{\circ} 30^{\circ})$, but not aligned with gas streamlines (***)
- ☐ Complicated spatial structures (e.g., magnetic arms), magnetised quasi-spherical halos, etc.
- ☐ <u>Misconception</u>: magnetic field in the Milky Way near the Sun is representative of all spiral galaxies: it is **NOT**



Face-on and edge-on views showing the evolution of the magnetic field in a model of the galaxy M83 (Brandenburg & Donner, from Beck et al., ARAA 1996)

Magnetic fields in spiral galaxies: summary

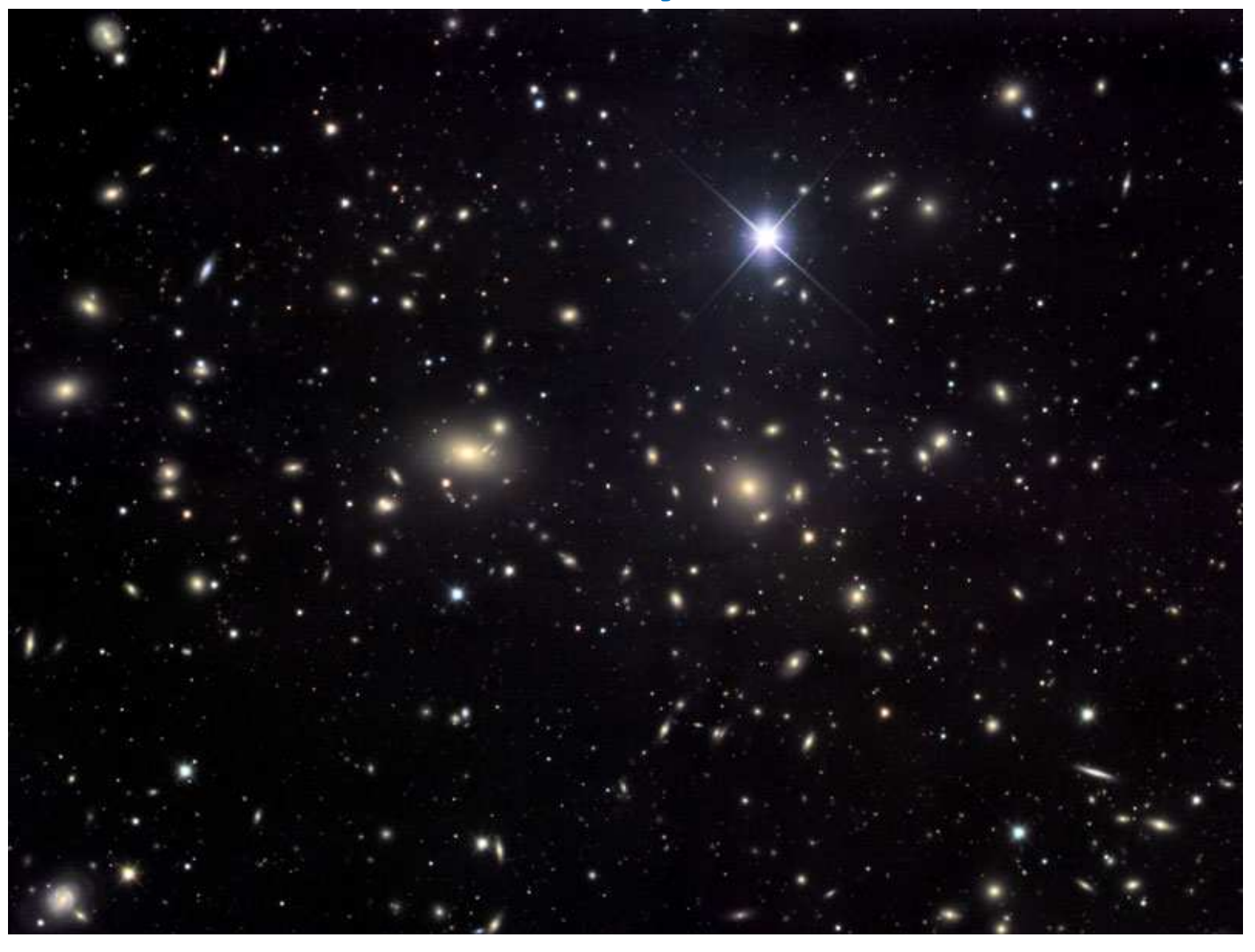
- \Box B=5-12 μG, $B_0=3-7$ μG, $b^2/B_0^2=3$, approximate equipartition with turbulent energy, $b \cong (4\pi\rho)^{1/2} v_0 \simeq 5 \mu$ G
- ☐ Quadrupolar global parity (**)
- Overall trailing spiral pattern, $\arctan B_r/B_\phi = -(10^{\circ} 30^{\circ})$, but not aligned with gas streamlines (***)
- ☐ Complicated spatial structures (e.g., magnetic arms), magnetised quasi-spherical halos, etc.
- ☐ <u>Misconception</u>: magnetic field in the Milky Way near the Sun is representative of all spiral galaxies: it is **NOT**



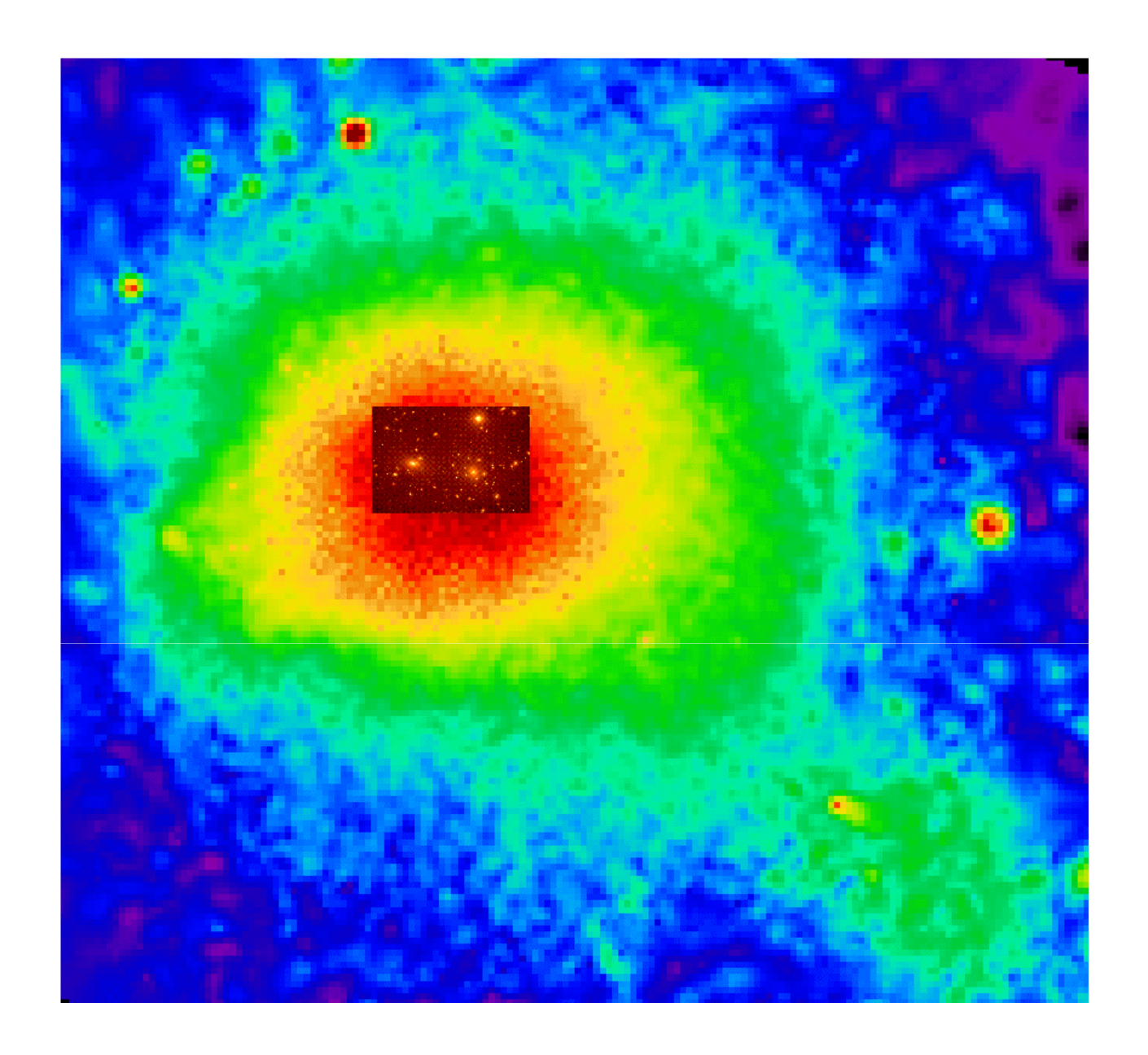
Magnetic fields in spiral galaxies: summary

- $\Box B = 5-12 \,\mu\text{G}, \quad B_0 = 3-7 \,\mu\text{G}, \quad b^2/B_0^2 = 3,$ approximate equipartition with turbulent energy, $b \cong (4\pi\rho)^{1/2} \, v_0 \simeq 5 \,\mu\text{G}$
- ☐ Quadrupolar global parity (**)
- Overall trailing spiral pattern, $\arctan B_{\gamma}/B_{\phi} = -(10^{\circ} 30^{\circ})$, but not aligned with gas streamlines (***)
- ☐ Complicated spatial structures (e.g., magnetic arms), magnetised quasi-spherical halos, etc.
- ☐ Misconception: magnetic field in the Milky Way near the Sun is representative of all spiral galaxies: it is NOT

2.2. Galaxy clusters



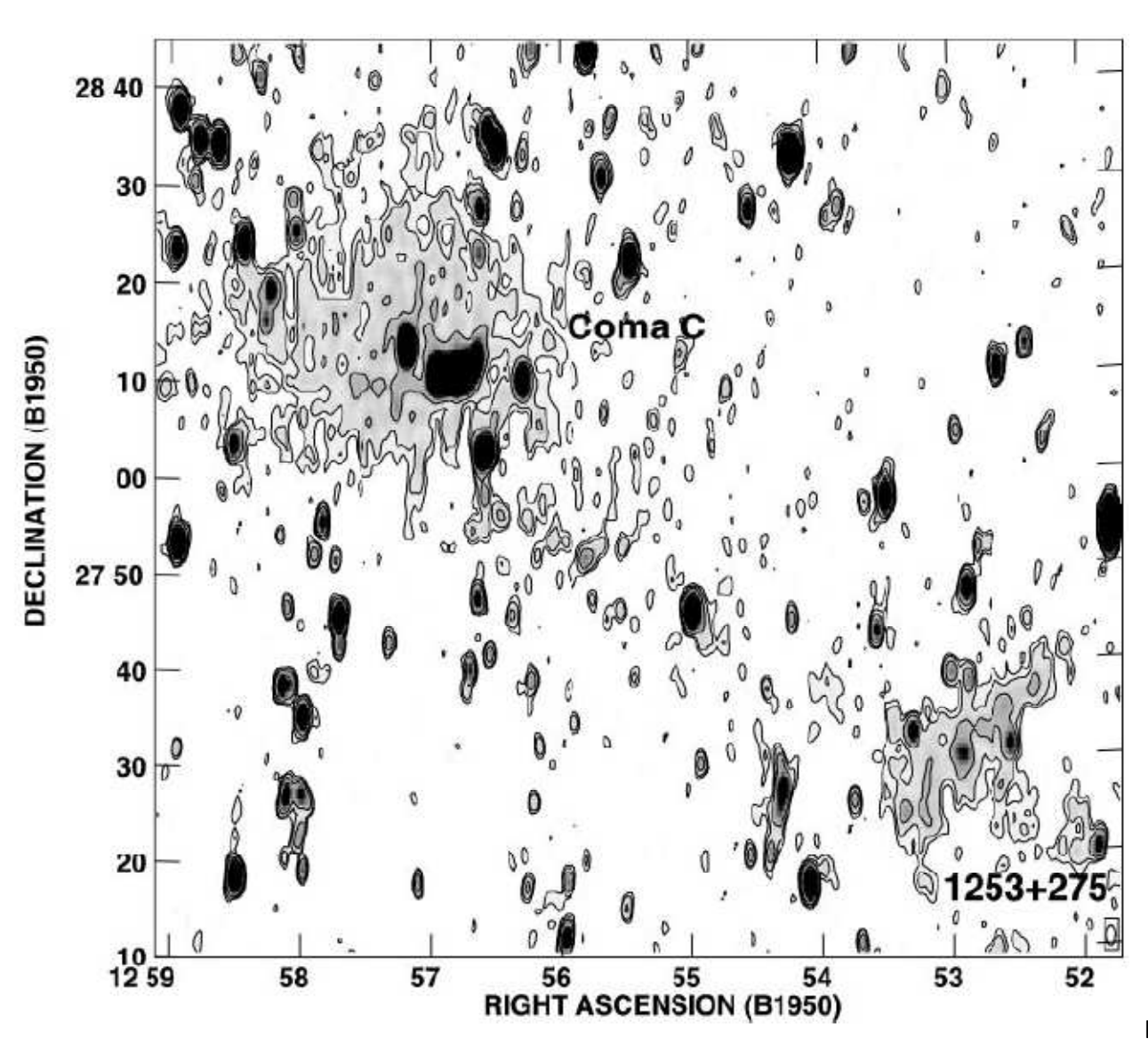
Coma cluster, central part, > 1000 galaxies (the Coma Berenices Constellation)



Coma cluster in X-rays (ROSAT): evidence for intergalactic gas

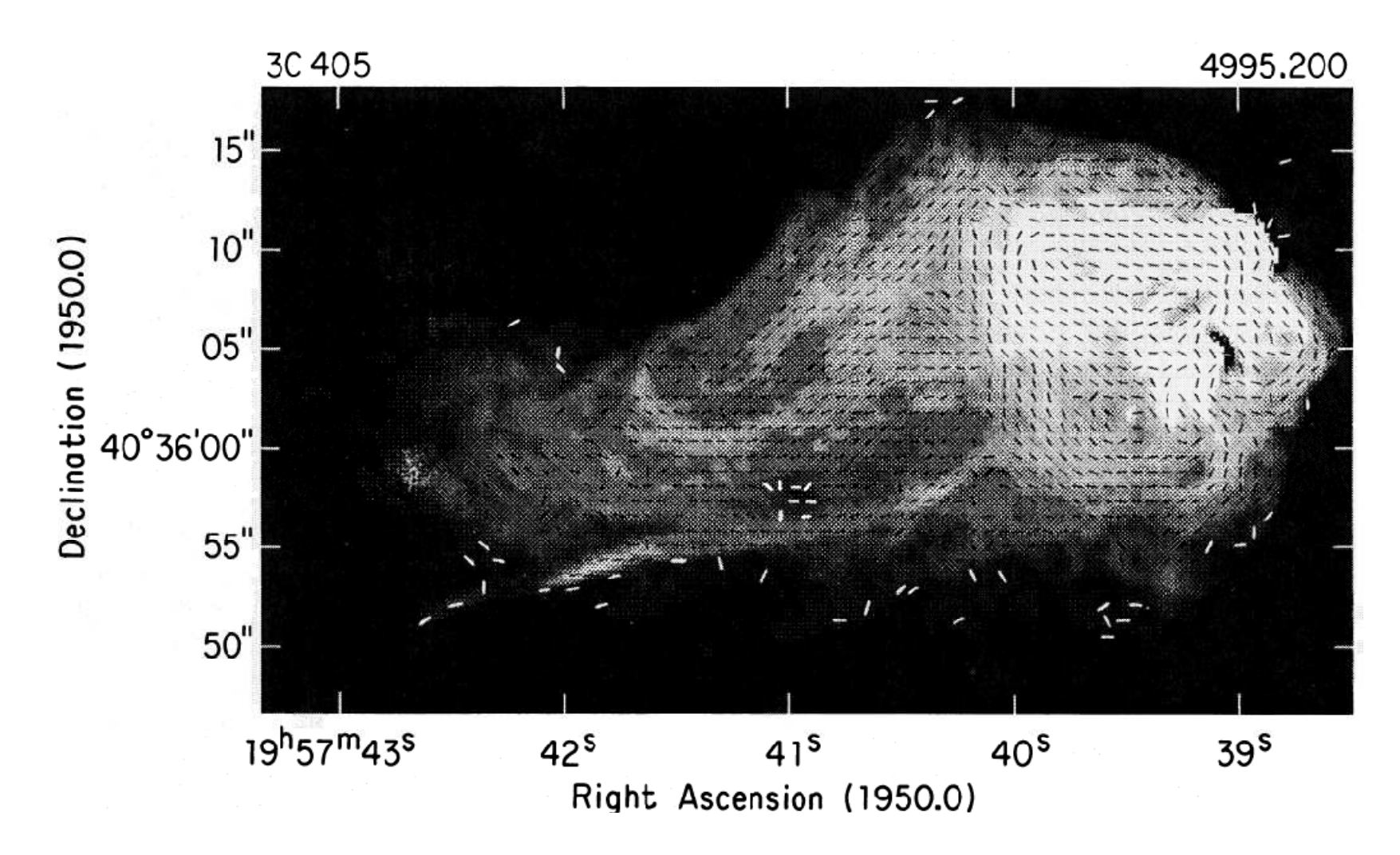
 $T = 10^6$ K, $n = 10^{-3}$ cm⁻³, R = 500 kpc, deviations from symmetry indicate recent merger

Radio halo: synchrotron emission of Coma at λ 90 cm



Feretti & Giovannini (1998), resolution 25×50 kpc (RA×DEC) .

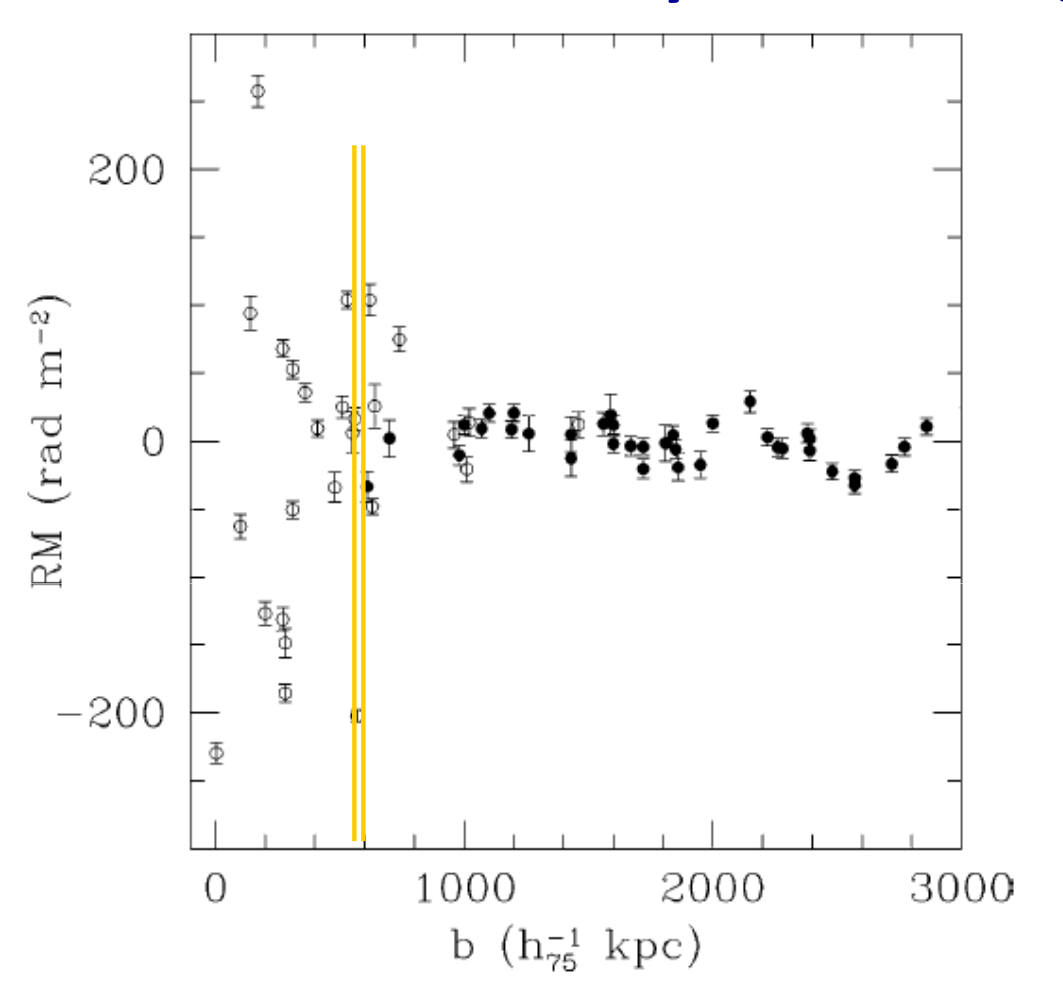
Faraday rotation in a cluster gas: radio lobes of Cyg A



Dreher et al., ApJ, 316, 611, 1987: magnetic field in the intracluster gas,

$$B = 2-10 \,\mu\text{G}, \quad l = 20-30 \,\text{kpc}$$

Faraday rotation in galaxy clusters



RM of background radio sources vs. distance from the cluster centre for 16 galaxy clusters;

filled symbols: field sources (Clarke et al., ApJ, 547, L111, 2001)

$$B = 2 \mu G$$
, $L = 500 \text{ kpc}$, $n_e = 10^{-3} \text{ cm}^{-3}$

$$\Rightarrow RM = 1000 \text{ rad/m}^2$$
$$= 10 \text{ RM}_{\text{observed}}$$

Random magnetic field b, scale $l_0 = 10 \text{ kpc}$:

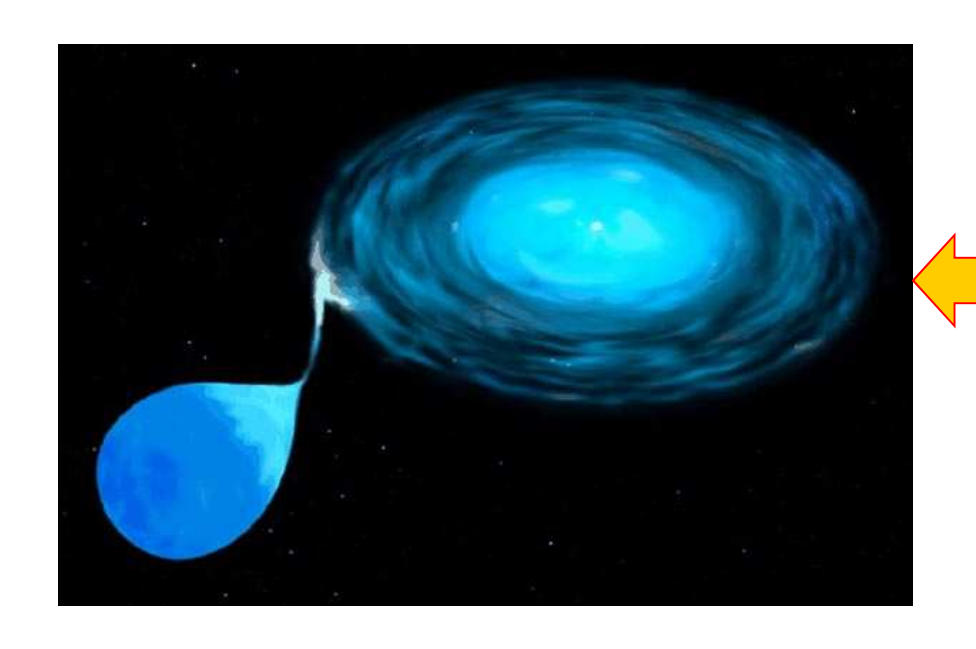
$$\sigma_{\rm RM} = 0.81 \ b n_{\rm e} (L l_0)^{1/2} = 100 \ {\rm rad/m^2} \Rightarrow b = 2 \ \mu {\rm G}$$

Observational estimates of magnetic fields in galaxy clusters

Method	Strength μ G	Model parameters
Synchrotron halos	0.4-1	Minimum energy, $k = \eta = 1$, $v_{\text{low}} = 10 \text{ MHz}$, $v_{\text{high}} = 10 \text{ GHz}$
Faraday rotation (embedded)	3-40	Cell size $= 10 \mathrm{kpc}$
Faraday rotation (background)	1-10	Cell size $= 10 \mathrm{kpc}$
Inverse Compton	0.2-1	$lpha = -1$, $\gamma_{\text{radio}} \sim 18000$, $\gamma_{\text{xray}} \sim 5000$
Cold fronts	1-10	Amplification factor \sim 3
GZK	> 0.3	AGN = site of origin for EeV CRs

2.3. Briefly on accretion discs

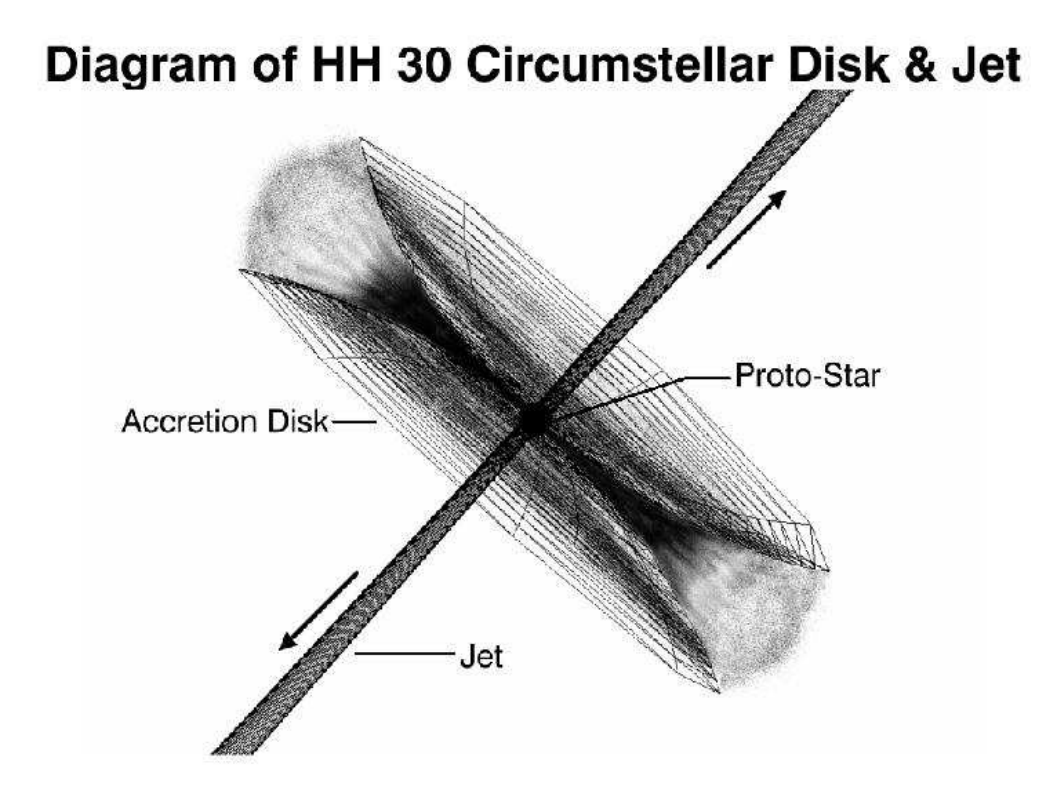
- □Occur in binary systems and around massive objects (compact stars, young stars, black holes)
- \square (Nearly) Keplerian rotation, $\Omega \propto r^{-3/2}$
- □Very thin
- □ Drive outflows and (magnetically?) collimate them into jets (young stars and active galaxies)
- ☐ Believed to be magnetised (to drive turbulence and outflows).



Binary stellar system



Young star HH 30





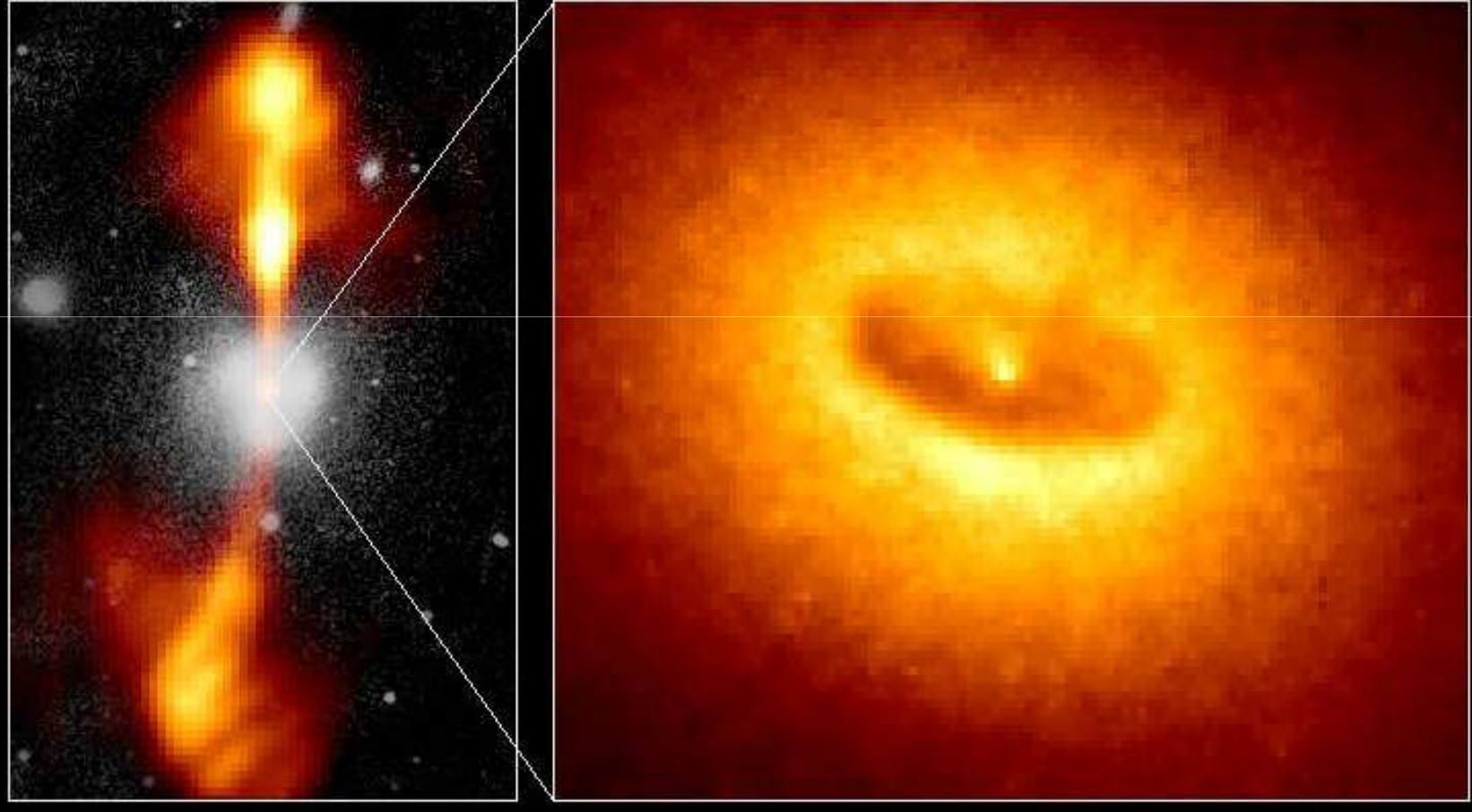
Core of Galaxy NGC 4261

Hubble Space Telescope

Wide Field / Planetary Camera

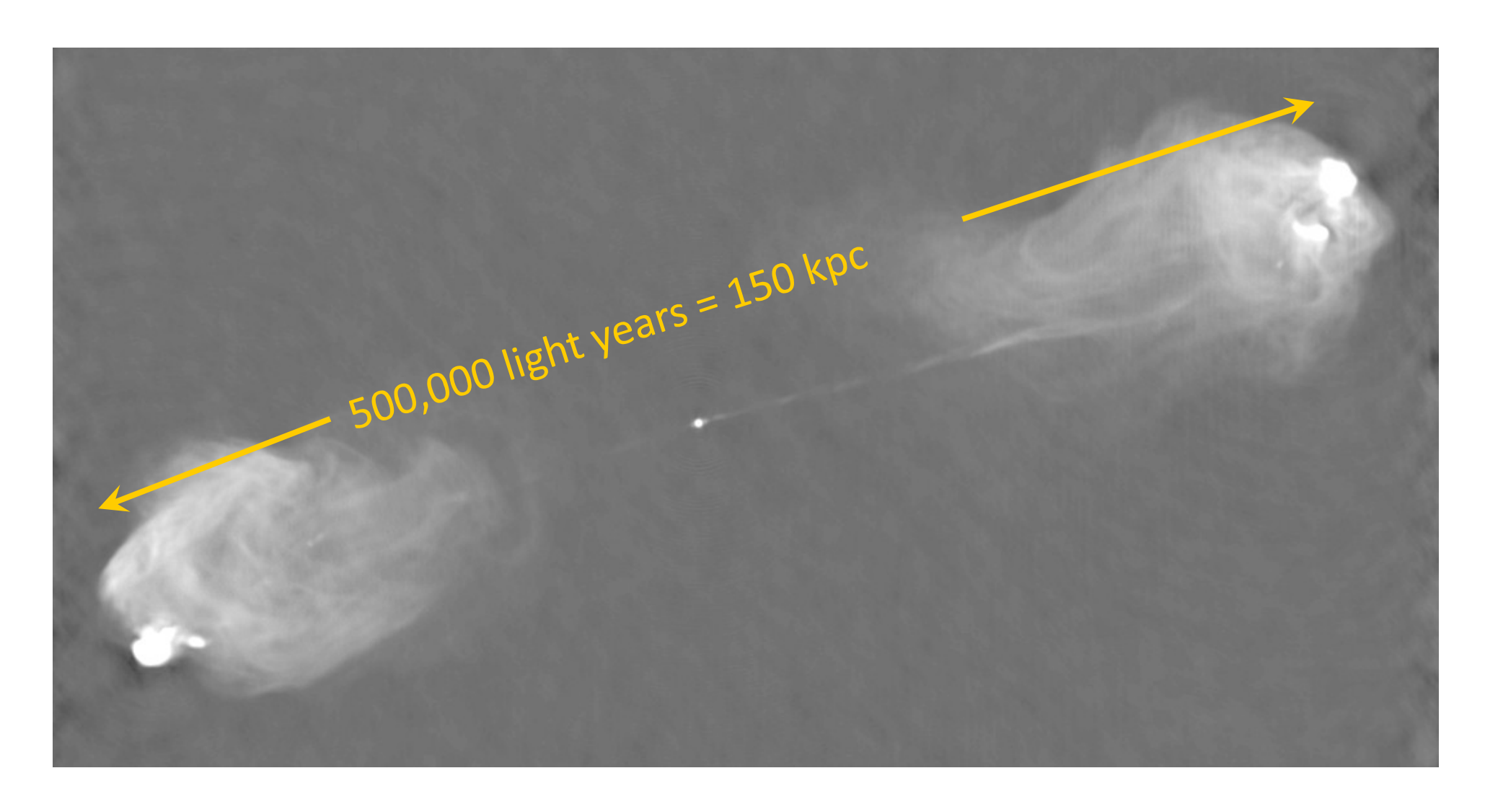
Ground-Based Optical/Radio Image

HST Image of a Gas and Dust Disk



380 Arc Seconds 88,000 LIGHTYEARS

1.7 Arc Seconds 400 LIGHT-YEARS



Radiogalaxy and jets, Cyg A at $\lambda 6$ cm (Taylor et al., ApJ, 463, 95, 1996)